Random-Finite-Set-Based Distributed Multirobot SLAM

Lin Gao, Giorgio Battistelli, and Luigi Chisci, *Senior Member, IEEE*

***Abstract*—This article addresses fully distributed multirobot (multivehicle) simultaneous localization and mapping (SLAM). More specifically, a multivehicle scenario is considered, wherein a team of vehicles explore the scene of interest in order to cooperatively construct the map of the environment by locally updating and exchanging map information in a neighborwise fashion. To this end, a random-set-based local SLAM approach is undertaken at each vehicle by regarding the map as a random finite set and updating the first-order moment, called probability hypothesis density (PHD), of its multiobject density. Consensus on map PHDs is adopted in order to spread the map information through the team of vehicles also taking into account the different and time-varying fields of view of the team members. The convergence of the consensus strategy is analyzed theoretically, and the effectiveness of the proposed approach is assessed on both simulated and experimental datasets. The complexity and scalability of the proposed approach are also analyzed both theoretically and experimentally.**

***Index Terms*—Consensus, probability hypothesis density (PHD), random finite set (RFS), robot navigation, sensor data fusion, simultaneous localization and mapping (SLAM).**

I. Introduction

SIMULTANEOUS localization and mapping (SLAM) consists of constructing in real time a map of the unknown environment surrounding an autonomous vehicle (mobile robot) while simultaneously estimating the vehicle motion within it [1]. SLAM has attracted a lot of attention owing to its wide potential applications in autonomous navigation [2] and driving [3], unfamiliar environment exploration [4], etc. According to the taxonomy in [14], the map can be represented in either occupancy-grid or landmark-based way, where the latter representation is considered in this article. In this setting, the landmark measurements are relative to the pose of the vehicle; thus, the localization error is deeply correlated with the mapping error. In the literature, landmark-based SLAM is commonly tackled within a probabilistic (Bayesian) framework [1], [6] as the determination of the joint distribution of the vehicle trajectory and the environment map conditioned on both sensor measurements and vehicle control inputs, referred to hereafter as the *joint posterior* (JP) distribution.

In the application of SLAM, it is convenient to factorize the JP *probability density function* (PDF) as the product of the conditional PDF of the map given the vehicle motion by the marginal PDF of the vehicle motion. Then, it turns out that the overall SLAM problem is decomposed into two subproblems: vehicle motion estimation and map estimation conditioned on the vehicle motion estimate. Such an idea has motivated two classes of SLAM algorithms, i.e., Rao–Blackwellized particle filtering SLAM (RBPF-SLAM) [7], among which a representative is FastSLAM [9], [10], and graph-based SLAM [8]. In this article, the attention is devoted to the former one, i.e., RBPF-SLAM. In RBPF-SLAM, vehicle motion estimation is usually accomplished via a particle filter (PF), where each particle represents a hypothesis for the vehicle pose evolution. Conversely, map estimation exhibits a very close resemblance with the multitarget tracking problem. At the present state of the art, there exist many SLAM approaches, in which data association between measurements and landmarks is explicitly considered [1], [9]–[13]. A survey on the state of the art can be found in [14]. More recently, it has been recognized that the map can actually be more naturally regarded as a *random finite set* (RFS) [16], [17] so that RFS multiobject filters, originally introduced for multitarget tracking purposes, have also been developed for SLAM [18]–[22]. The advantage of the RFS approach over the traditional one is that it can incorporate data association, landmark appearance and disappearance, missed detections, and false alarms in the Bayesian recursion, so that the JP can be propagated in a more elegant and effective way.

It has been recognized that utilizing several vehicles to cooperatively explore the area of interest can enhance both efficiency and performance of SLAM [5], [23], [24]. One of the major extra challenges of multivehicle SLAM (MV-SLAM) over single-vehicle SLAM (SV-SLAM) lies in the problem of map fusion [5]. Actually, if the maps are not fused in a proper manner, the overall performance of mapping will possibly degrade compared to the single vehicle mapping and then affect the performance of vehicle motion estimation. Generally speaking, the local maps from multiple vehicles can be fused either in a centralized way, where the global map is constructed by carrying out fusion at the likelihood level, or in a distributed way, where the global map is constructed by fusing the local maps of vehicles. Because of the fact that distributed systems have

Manuscript received October 31, 2019; revised February 19, 2020; accepted June 9, 2020. Date of publication July 2, 2020; date of current version December 3, 2020. This work was supported by Fondazione CR Firenze. This article was recommended for publication by Associate Editor A. Franchi and Editor P. Robuffo Giordano upon evaluation of the reviewers' comments. *(Corresponding author: Giorgio Battistelli.)*

The authors are with the Dipartimento di Ingegneria dell'Informazione, Università degli Studi di Firenze, 50134 Florence, Italy (e-mail: lin.gao@unifi.it; giorgio.battistelli@unifi.it; luigi.chisci@unifi.it).

Color versions of one or more of the figures in this article are available online at http://ieeexplore.ieee.org.

Digital Object Identifier 10.1109/TRO.2020.3001664

1552-3098 © 2020 IEEE. Personal use is permitted, but republication/redistribution requires IEEE permission.
See https://www.ieee.org/publications/rights/index.html for more information.

Authorized licensed use limited to: Universita degli Studi di Firenze. Downloaded on January 27,2025 at 10:15:12 UTC from IEEE Xplore. Restrictions apply.

remarkable advantages in terms of low communication load, flexibility, and scalability [43], it is of particular importance to develop a fully distributed MV-SLAM (DMV-SLAM) filter.

In this article, we consider a multivehicle scenario, wherein multiple vehicles cooperatively explore different, typically overlapping, portions of a given environment with the aim to construct a map of the overall environment. It is assumed that vehicles can communicate with each other depending on their relative position, and that there is no master vehicle that can gather all the information from the other (slave) vehicles, so that all vehicles must cooperate in a peer-to-peer fashion in order to solve the SLAM problem. To this end, the RFS paradigm is followed, and the probability hypothesis density (PHD) representation [44] is specifically adopted for the map RFS. Kullback–Leibler fusion (KLF) [45] and consensus of PHDs [46] are exploited for fusing multiple PHDs in a distributed peer-to-peer manner. Unlike multitarget tracking addressed in [46], however, the MV-SLAM problem of this article is characterized by different and time-varying fields of view (FoVs). Hence, a direct application of the fusion method of [46] to standard PHD-SLAM [18]–[21] is ruled out, since the resulting fused map PHD would be null outside the common FoV of vehicles.

In this article, the problem of fusing map PHDs among agents with different time-varying FoVs is solved by combining KLF with the so-called *adaptive birth method* (ABM) [48], [49]. In single-vehicle PHD-SLAM, the ABM is usually employed in order to initialize new components in the PHD map on the basis of the collected measurements, so as to account for newly appeared or previously undetected landmarks. In this article, the ABM is extended to the multivehicle case so that each vehicle is able to initialize new components from neighbors in the fusion steps. Furthermore, in the map fusion step, it is proposed that just a single estimated (unconditional) map PHD of each vehicle be passed over the network in order to perform map consensus, while multiple maps conditioned on several vehicle trajectories are locally managed by each vehicle. In this respect, a mathematical analysis on convergence as well as optimality of the proposed method is carried out. Moreover, an efficient *Gaussian mixture* (GM) implementation is proposed to perform DMV-SLAM. In the proposed implementation, the map PHD of each vehicle before fusion is represented as an affine GM, i.e., a GM plus a constant that models the fact that new landmarks can be discovered in the whole map space with uniform probability. Before map fusion with a neighboring vehicle, it is split into two parts: one, called matched GM, containing all *Gaussian components* (GCs) that are sufficiently close (in Mahalanobis distance) to some GC of the other fusing map and the other, complementary, unmatched GM. Then, the matched GMs are directly fused according to KLF, while the remaining unmatched GMs of both vehicles are fused only with the constant component and added. The effectiveness of the proposed algorithm is assessed with both simulated and experimental datasets [50], [51]. Some videos showing the evolution over time of DMV-SLAM can be found in [52].

The main contributions of this article can be summarized as follows.

1) A new ABM is proposed for PHD-SLAM that makes it possible to initialize new landmarks from neighbors in the fusion steps.
2) Based on such ABM as well as the consensus diffusion strategy, a fully distributed MV-PHD-SLAM (DMV-PHD-SLAM) algorithm is proposed.
3) A computationally efficient implementation strategy of the proposed DMV-PHD-SLAM algorithm is provided, and its computational complexity and memory occupation are analyzed.

II. Related Work

DMV-SLAM has been investigated by several researchers in the past decade. In [25], DMV-SLAM was tackled by regarding the estimated landmark positions from neighbor vehicles as additional virtual measurements. This approach was also extended to the case of unknown relative initial poses among vehicles by forcing all vehicles to explore common landmarks. In [33], based on the assumption that all landmarks have globally unique identifiers (i.e., no data association is needed), the authors extended to the multivehicle case the smoothing and mapping graphical model approach of [34] by introducing the constrained factor graph as an extended graphical model in order to perform map fusion. Such a method suffers from the problem of double counting and was then fixed in [35] by combining local and neighborhood information into a single augmented local map. In [36], a decentralized localization algorithm was presented in order to work in dynamic robot networks without full-connectivity requirements. Each robot only needs to consider its own knowledge of the network topology in order to get localization performance equivalent to the centralized case whenever possible. Based on such a method, Leung *et al.* [37] proposed a novel graph-based framework for DMV-SLAM that does not rely on any specific local SLAM method. Guo *et al.* [38], based on the assumption that the relative initial poses among vehicles are known, studied the problem of cooperative mapping, wherein the local trajectory and map of each vehicle are combined into a global map by imposing geometric constraints among jointly observed point and line features.

Besides the aforementioned contributions, there has also been a lot of work closely related to DMV-SLAM. For instance, in [23] and [26]–[32], the problem of centralized MV-SLAM was successfully addressed. In [39] and [40], a distributed strategy was proposed to handle the problem of feature map fusion, which consists of two main tasks, i.e., association and state fusion. Such a strategy can work with traditional divide-and-conquer SLAM algorithms (e.g., EKF-SLAM and FastSLAM) that directly output map estimates, while it is unsuitable for density-based map estimation algorithms. Paull *et al.* [41] addressed the problem of path planning of multiple vehicles for area coverage, which can be regarded as an inspiration for the problem of DMV-SLAM. The problem of 2-D grid-map fusion has been addressed in [42], which can be further extended to DMV-SLAM with grid maps.

Preliminary results on DMV-PHD-SLAM can be found in [47], where it was proposed to solve the problem of fusing

Authorized licensed use limited to: Universita degli Studi di Firenze. Downloaded on January 27,2025 at 10:15:12 UTC from IEEE Xplore. Restrictions apply.

map PHDs among vehicles with different FoVs by initializing each SLAM agent by an uninformative (flat) map PHD, which is approximately represented by a GM containing a large number of GCs. In this way, the map PHD outside the FoV of each vehicle is no longer null, and landmarks outside the common FoV could be properly preserved after KLF. However, this preliminary solution suffered from two major drawbacks: 1) it requires heavy computational burden; and 2) it works well only when the probability of landmark detection is sufficiently high (close to 1) for each vehicle; otherwise, the PHD of an agent tends to become extremely small (even null because of the pruning strategy adopted to limit the computational load) in correspondence of landmarks that have not been detected by such an agent when the landmark was in its FoV. As a result, when performing fusion with other vehicles, such landmarks have a very high probability of being lost. In this article, a novel ABM is proposed, where the GCs of the birth PHD are created only at locations where there is high probability of having landmarks. Moreover, the fusion strategy is tailored so as to take into consideration the prior knowledge of the expected number of landmarks per unit volume of the map space. The proposed method avoids resorting to the uninformative initial PHD and thus provides significant reduction of both computational load and memory occupancy.

III. RFS-Based SV-SLAM

The aim of this section is to recall the random set approach to SV-SLAM [18], [20], which is referred to as PHD-SLAM in this article. It should be clarified that, since the PHD-SLAM algorithm is not vehicle dependent, all the variables are not tied to any specific vehicle in this section.

A. Problem Formulation

Let $\mathbb{X}$ denote the space of all possible poses of the autonomous vehicle (mobile robot) and $x_{0:t} = \{x_0, x_1, \ldots, x_t\} \in \mathbb{X}^{t+1}$ the vehicle trajectory, i.e., the sequence of poses up to time t. It is supposed that the vehicle can predict its motion by means of a dynamical model with known input u_t in the short term. Accordingly, $u_{0:t} = \{u_0, u_1, \ldots, u_t\}$ denotes the sequence of control inputs. Hence, the time evolution of the vehicle relies on the following motion model:

$$x_t = f_t\left(x_{t-1}, u_{t-1}, w_t\right) \tag{1}$$

where w_t is the so-called process noise. In this article, the map of the environment is described as a set of fixed (motionless) point landmarks, represented as vectors in a suitable *map space* $\mathbb{M}$, that can be detected by the sensors onboard the vehicles. Hence, the visited map $\mathcal{M}_t$ consists of a finite subset of $\mathbb{M}$, whose cardinality and elements are both unknown.

At each time t, each vehicle acquires measurements about its surroundings. These raw data are fed into a suitable feature extraction algorithm, whose role is to identify the landmarks. The output of this algorithm lives in a suitable measurement space $\mathbb{Z}$ that depends on the types of sensors onboard the vehicle. When a landmark m is detected by the vehicle, a measurement z is generated with probability described by the single-object likelihood function $g_t(z|m, x_t)$.

Because of the fact that any practical feature extraction algorithm is imperfect, the presence of false measurements (i.e., measurements not belonging to any landmark) as well as the possibility of miss-detections (i.e., existing landmarks that do not generate any measurement) must be taken into account. At each time t, the output of the feature extraction algorithm is a finite set of measurements $\mathcal{Z}_t \subset \mathbb{Z}$, and accordingly, $\mathcal{Z}_{0:t} = \{\mathcal{Z}_0, \mathcal{Z}_1, \ldots, \mathcal{Z}_t\}$ denotes the sequence of observations collected up to time t.

B. Outline of the Single-Vehicle PHD-SLAM Algorithm

In this article, the unknown map $\mathcal{M}$ is modeled as an RFS, i.e., a set that is random in both the number of elements (i.e., the number of landmarks) and the values of the elements (i.e., the landmark locations). The basics of RFS theory needed to develop the proposed SLAM algorithm are briefly reviewed in Appendix A; details can be found in [16].

From a Bayesian viewpoint, solving SLAM amounts to propagating the JP

$$p_{t|t}(\mathcal{M}_t, x_{0:t}) \triangleq p_{t|t}(\mathcal{M}_t, x_{0:t}|\mathcal{Z}_{0:t}, u_{0:t-1}, x_0). \tag{2}$$

Note that such a PDF is a hybrid one, being the joint PDF of a random set (the map $\mathcal{M}_t$) and an ordinary random vector (the trajectory $x_{0:t}$). In principle, Bayesian SLAM can be carried out via a slight modification of the multiobject Bayes filter, so as to account for such a hybrid nature [19]. However, the aforementioned recursion involves multiple ordinary and set integrals, which hinder a direct algorithmic implementation. PHD-SLAM circumvents such difficulties by factoring the SLAM posterior PDF into the product of a multiobject PDF and an ordinary PDF

$$\begin{aligned} p_{t|t}\left(\mathcal{M}_t, x_{0:t}\right) &= p\left(\mathcal{M}_t \middle| x_{0:t}, \mathcal{Z}_{0:t}\right) p\left(x_{0:t} \middle| \mathcal{Z}_{0:t}, u_{0:t}, x_0\right) \\ &\triangleq p_{t|t}\left(\mathcal{M}_t \middle| x_{0:t}\right) p_{t|t}\left(x_{0:t}\right). \end{aligned} \tag{3}$$

Such a factorization makes it possible to adopt a PF to propagate the marginal trajectory PDF, which is then approximated as

$$p_{t|t}(x_{0:t}) \approx \sum_{i=1}^{M} \omega_t^i \, \delta(x_{0:t} - \widehat{x}_{0:t}^i) \tag{4}$$

where $\delta(\cdot)$ represents the Dirac delta and ω_t^i are nonnegative importance weights summing up to unity, i.e., $\sum_{i=1}^{M} \omega_t^i = 1$. For each trajectory hypothesis $\widehat{x}_{0:t}^i$ maintained by the PF, the multiobject PDF of the map conditioned on such hypothesis is modeled as a Poisson RFS represented by means of its PHD, denoted by $D_{t|t}^i(m|\widehat{x}_{0:t}^i)$ (and abbreviated as $D_{t|t}^i(m)$ hereafter). The PHD $D_{t|t}^i(m)$ can be interpreted as the local expected density of landmarks at point m so that the peaks of the PHD correspond to the most probable locations of the landmarks (a sample of PHD over a $[0\ 600] \times [0\ 600]$ $[\mathrm{m}^2]$ region is illustrated in Fig. 1). The reader is referred to Appendix A for a brief review of the PHD. Summing up, a different conditional map PHD $D_{t|t}^i(m)$ is maintained for each particle $i = 1, \ldots, M$ and propagated via a PHD filter.

Authorized licensed use limited to: Universita degli Studi di Firenze. Downloaded on January 27,2025 at 10:15:12 UTC from IEEE Xplore. Restrictions apply.

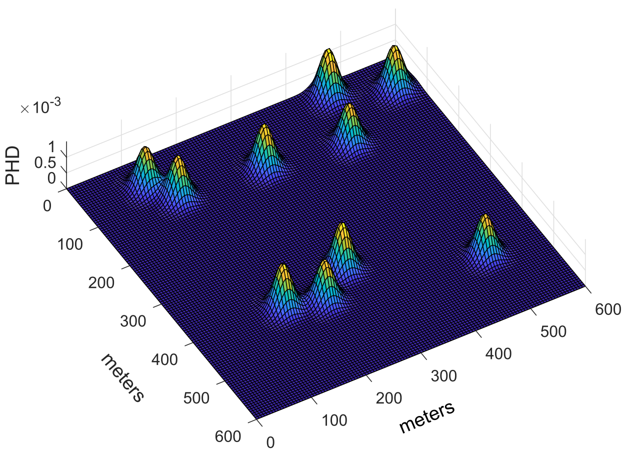

Fig. 1. Example of PHD.

As a result, the PHD-SLAM algorithm propagates a set of extended particles $\mathcal{P}_t = \{\mathcal{P}_t^i\}_{i=1}^M$, each one consisting of an importance weight, a trajectory hypothesis, and a PHD, i.e.,

$$\mathcal{P}_t^i = \{\omega_t^i, \widehat{x}_{0:t}^i, D_{t|t}^i(\cdot)\}. \tag{5}$$

As expected, the trajectory PF and the map PHD filter are not independent of each other. Indeed, the map PHD plays its role inside the particle weight update (correction) step, which, if the dynamic prior is used as PF proposal density, takes the following form:

$$\omega_t^i = \frac{\zeta\left(\mathcal{Z}_t|\mathcal{Z}_{1:t-1}, \widehat{x}_{0:t}^i\right)}{\sum_{j=1}^M \omega_{t-1}^j \zeta\left(\mathcal{Z}_t|\mathcal{Z}_{1:t-1}, \widehat{x}_{0:t}^j\right)}\omega_{t-1}^i \tag{6}$$

where $\zeta(\mathcal{Z}_t|\mathcal{Z}^{t-1}, \widehat{x}_{0:t}^i)$ represents the multiobject likelihood. The likelihood $\zeta(\mathcal{Z}_t|\mathcal{Z}^{t-1}, \widehat{x}_{0:t}^i)$ can be computed with different methods in the framework of PHD-SLAM. For instance, it can be specified to the *empty map* [18, eq. (26)] or *single-feature map* [18, eq. (27)] or *multifeature map* [15, eq. (28)] based on the Rao–Blackwellized PHD filter, or it can be also computed in the context of the single-cluster PHD filter [20, eq. (34)]. Since this article does not actually focus on the development of the single-vehicle PHD-SLAM filter but rather on the map fusion, details on the computation of the likelihood are out of the scope of this article.

Given the particle set $\mathcal{P}_t$, the vehicle pose and the map can be estimated using either the *expected a posteriori* (EAP) or *maximum a posteriori* (MAP) criteria.

According to the EAP criterion, the minimum mean square error (MMSE) estimate of the vehicle pose at time t is approximated as

$$\widehat{x}_{t|t} = \sum_{i=1}^M \omega_t^i \, \widehat{x}_t^i. \tag{7}$$

As far as the map is concerned, the quantity of interest is the unconditional PHD of the random set $\mathcal{M}_t$, which is denoted by $\widehat{D}_{t|t}(\cdot)$. The following result holds:

$$\widehat{D}_{t|t}(m) = \mathrm{E}_{x_{0:t}}[D_{t|t}(m|x_{0:t})] \tag{8}$$

where $E_{x_{0:t}}$ denotes the expectation operator over the distribution of $x_{0:t}$. Hence, such unconditional PDF can be approximated as

$$\widehat{D}_{t|t}(m) = \sum_{i=1}^M \omega_t^i \, D_{t|t}^i(m). \tag{9}$$

According to the MAP criterion, the particle with highest weight is considered, i.e.,

$$i^* \in \arg \max_{i=1,\ldots,M} \omega_t^i. \tag{10}$$

Then, the MAP estimate of the vehicle pose is taken as

$$\widehat{x}_{t|t} = \widehat{x}_t^{i^*} \tag{11}$$

and the map is estimated by considering the conditional MAP PHD

$$\widehat{D}_{t|t}(m) = D_{t|t}^{i^*}(m)\,. \tag{12}$$

Once the PHD $\widehat{D}_{t|t}(m)$ has been determined using either (9) or (12), the estimates of the landmark locations in the space $\mathbb{M}$ can be obtained by extracting the most significant peaks of $\widehat{D}_{t|t}(m)$.

C. *Propagation of the Conditional PHD*

The crucial point of PHD-SLAM is to propagate, at each time t, the conditional PHDs $D_{t|t}^i(\cdot)$ $(i = 1, \ldots, M)$ of all particles. Since this involves computation of integrals through the PHD recursions, it is impossible to propagate the PHD in closed form. Conditional PHDs are usually approximated by GMs[1] [57], i.e.,

$$D_{t|t}^i(m) = \sum_{k=1}^{J_t^i} \alpha_t^{i,k} \mathcal{G}\left(m; \widehat{m}_t^{i,k}, P_t^{i,k}\right) \tag{13}$$

where $\mathcal{G}(m; \widehat{m}, P)$ denotes the Gaussian PDF with mean $\widehat{m}$ and covariance P.

The PHD filter consists of two steps, prediction and correction, that are carried out independently for each particle (i.e., trajectory hypothesis). In the prediction step of PHD-SLAM, the predicted conditional PHD $D_{t|t-1}^i(m)$ is obtained by adding the so-called *birth density* $B_t^i(m)$ to the conditional PHD $D_{t-1|t-1}^i(m)$, i.e.,

$$D_{t|t-1}^i(m) = D_{t-1|t-1}^i(m) + B_t^i(m)\,. \tag{14}$$

The birth density $B_t^i(m)$ accounts for newly appeared or previously undetected landmarks. A typical choice for the birth density $B_t^i(m)$ is the so-called ABM [48], [49], in which new GCs are generated from the measurements collected at time $t-1$. Note that, since the primary concern here is on the map fusion between agents with different FoVs, this article considers, for the sake of simplicity, a purely static map, wherein all landmarks are motionless. In the general case of mobile landmarks, (14) could be modified so as to account for landmark motion [20].

[1]Another representation of PHDs is by means of particles [54]. However, this method requires higher computational burden not affordable in the context of PHD-SLAM.

Authorized licensed use limited to: Universita degli Studi di Firenze. Downloaded on January 27,2025 at 10:15:12 UTC from IEEE Xplore. Restrictions apply.

Algorithm 1: PHD-SLAM Filter (Time t).

Input: $\mathcal{P}_{t-1}$ and $\mathcal{Z}_t$

1: Predict the conditional PHD of each particle via (14);
2: For $i = 1, \ldots, M$, sample the new trajectory hypothesis $\widehat{x}_t^i$ from $\widehat{x}_{t-1}^i$ via a suitable importance sampling distribution [58];
3: Compute the updated conditional PHD of each particle $D_{t|t}^i$ via (16);
4: Reweight particles and then normalize particle weights by (6);
5: Estimate the vehicle pose using either the MAP or EAP strategy;
6: Compute the estimated PHD $\widehat{D}_{t|t}$ from $\{D_{t|t}^i\}_{i=1}^{M_r}$ using either the MAP or EAP strategy;
7: Extract the landmarks (i.e., the estimated map $\widehat{\mathcal{M}}_t$) from $\widehat{D}_{t|t}$;
8: Resample [59] to the new set of particles $\mathcal{P}_t^i$, $i = 1, \ldots, M$.

Output: $\mathcal{P}_t$, $\widehat{x}_{t|t}$, and $\widehat{\mathcal{M}}_t$

Let $P_D(m|x_t)$ be the probability of detecting a landmark located at m given that the pose of the vehicle is x_t. This clearly implies that the vehicle FoV at time t can be defined as

$$\mathcal{V}_t = \{m \in \mathbb{M} \,| P_D(m|x_t) > 0\}. \tag{15}$$

Furthermore, let $\kappa(z|x_t)$ be the intensity of false measurements (clutter) in the map space $\mathbb{M}$ given the vehicle pose. Then, the correction step of PHD-SLAM takes the form

$$\begin{aligned} D_{t|t}^i(m) &= \left[1 - P_D\left(m|\,\widehat{x}_t^i\right)\right] D_{t|t-1}^i(m) \\ &+ \sum_{z \in \mathcal{Z}_t} \frac{P_D\left(m|\,\widehat{x}_t^i\right) g_t(z|m, x_t^i) D_{t|t-1}^i(m)}{\kappa(z|x_t) + \int P_D\left(m|\,\widehat{x}_t^i\right) g_t(z|m, x_t^i) D_{t|t-1}^i(m) dm} \end{aligned} \tag{16}$$

also called PHD update equation. Note that the equivalence between the updated PHDs and the predicted PHDs of the landmarks outside the FoV is guaranteed by the fact that $P_D(m|x_t) = 0$ for $m \notin \mathcal{V}_t$. Hence, GCs corresponding to landmarks outside the FoV do not change during correction. Conversely, the PHD inside the FoV is modified on the basis of the measurements collected at time t. It should be noted that, in practice, the FoV $\mathcal{V}_t$, measurement noise variance, and clutter intensity $\kappa(\cdot|\cdot)$ may not be known precisely. In such a case, the method of robust PHD filtering in [55] and [56] can be exploited. The details of practically dealing with the FoV are deferred to [20, Sec. II-B].

Details on the GM implementation of the correction step can be found in [57]. Note that the number of GCs increases by a factor $|\mathcal{Z}_t|$ after each update step, which will eventually lead to an unacceptable computational load. Hence, a suitable procedure to limit the number of GCs needs to be adopted. This can be accomplished, e.g., by the *pruning & merging* methods described in [57, Table II]. The overall PHD-SLAM filter is summarized by Algorithm 1.

IV. Distributed Multiobject Fusion Over a Peer-to-Peer Network

The aim of this section is to introduce background on distributed multiobject estimation over a static peer-to-peer network, though the results can be extended to time-varying networks as well. Let $(\mathcal{N}, \mathcal{A})$ be a network with stationary agents, where $\mathcal{N} = \{1, \ldots, N\}$ is the vehicle set and $\mathcal{A} \subseteq \mathcal{N} \times \mathcal{N}$ the arc set, i.e., $(r, s) \in \mathcal{A}$ if and only if vehicle r can receive data from vehicle s. It is also assumed that the network works in a peer-to-peer fashion, i.e., all vehicles operate in the same way exchanging data with the neighbors, and there is no fusion center. Moreover, let $\mathcal{N}^r$ denote the in-neighborhood of vehicle $r \in \mathcal{N}$ (i.e., the set of vehicles from which r receives data). Assume the vehicles to be associated with suitable, possibly multiobject, densities $p^r(\mathcal{M}) \triangleq p(\mathcal{M}|\mathcal{Z}^r)$ relative to a common RFS of interest $\mathcal{M}$, obtained from possibly correlated measurement sets $\mathcal{Z}^r$.

The purpose is to compute, in each vehicle $r \in \mathcal{N}$, the collective (fused) density $\bar{p}(\mathcal{M})$, which takes into account the whole information gathered over the network. In this article, the fused density $\bar{p}(\mathcal{M})$ is taken as the weighted normalized geometric mean

$$\bar{p}\left(\mathcal{M}\right) = \frac{\prod_{r \in \mathcal{N}} \left[p^r\left(\mathcal{M}\right)\right]^{\pi^r}}{\int \prod_{r \in \mathcal{N}} \left[p^r\left(\mathcal{M}'\right)\right]^{\pi^r} \delta \mathcal{M}'} \tag{17}$$

where π^r are suitable nonnegative weights summing up to unity, and the integral in (17) has to be intended in the set integral sense. The fusion rule (17) was originally proposed for the fusion of PDFs in the statistics literature, where it is known as *logarithmic opinion pool* [61]. Its generalization to RFS densities was first proposed in [62] as *generalized covariance intersection* (GCI). As discussed in [46], the fusion rule (17) admits a meaningful information-theoretic interpretation as *weighted Kullback–Leibler average* (wKLA) of the densities to be fused. In particular, when $\pi^r = \frac{1}{N}$ for all $r \in \mathcal{N}$, $\bar{p}(\mathcal{M})$ turns out to be the unweighted Kullback–Leibler average (KLA). The fusion rule (17) has been shown to be immune to double counting of information [60], [62].

In case that the local map at each vehicle r is a multiobject Poisson process with PHD $D^r(m)$, then the collective map resulting from (17) turns out to be of the same type, with PHD $\bar{D}(m)$ given by [63]

$$\bar{D}(m) = \prod_{r \in \mathcal{N}} \left[D^r(m)\right]^{\pi^r}. \tag{18}$$

Normally, however, a vehicle r cannot access the local PHDs of all other vehicles. In order to overcome this limitation, a consensus approach [46] is adopted to compute the unweighted collective PHD $\bar{D}(m)$ at each vehicle by iterating several times data exchanges with the neighbors and wKLA of the received PHDs with the local one. Specifically, whenever the local PHD $D^r(m)$ has been obtained at vehicle $r \in \mathcal{N}$ after the local PHD filtering step, the fused PHD $\bar{D}^r(m)$ is computed by the following steps.

1) Before consensus, set $D_0^r(m) = D^r(m)$.

Authorized licensed use limited to: Universita degli Studi di Firenze. Downloaded on January 27,2025 at 10:15:12 UTC from IEEE Xplore. Restrictions apply.

2) For $\ell = 1, \dots, L$ broadcast $D^r_{\ell-1}(m)$ to the out-neighbors and receive $D^s_{\ell-1}(m)$, $s \in \mathcal{N}^r$, from the in-neighbors. Then, perform the consensus step

$$D^r_\ell(m) = \prod_{s \in \mathcal{N}^r \cup \{r\}} \left[D^s_{\ell-1}(m) \right]^{\pi^{rs}} \tag{19}$$

where $\pi^{rs} > 0$ are suitable consensus weights such that $\pi^{rr} + \sum_{s \in \mathcal{N}^r} \pi^{rs} = 1$.

3) After consensus, set $\bar{D}^r(m) = D^r_L(m)$.

Remark 1: Under suitable network connectivity conditions and choices of the consensus weights, it turns out that $\bar{D}^r(m)$ converges to the unweighted collective PHD [45] when $L \to \infty$, i.e.,

$$\lim_{L \to \infty} D^r_L(m) = \bar{D}(m) \tag{20}$$

for any vehicle r. A sufficient condition for (20) is that the matrix Π of the consensus weights be primitive (i.e., there exists an integer $\ell > 0$ such that each entry of Π^ℓ is strictly positive) and doubly stochastic (i.e., both its rows and columns sum up to unity). Furthermore, Π turns out to be primitive whenever the underlying network $(\mathcal{N}, \mathcal{A})$ is strongly connected. When the network is undirected, a possible choice ensuring double stochasticity of Π is given by the so-called Metropolis weights [64]. Another typical choice [65] amounts to setting $\Pi = I - \epsilon\Lambda$, where Λ is the network Laplacian and ϵ a positive scalar; indeed, such a matrix turns out to be primitive for suitably small values of ϵ and doubly stochastic for any balanced network. Note that the convergence in (20) has to be intended in the pointwise sense, but under mild assumptions (i.e., boundedness of all local PHDs $D_r(m)$), uniform convergence also holds. The above convergence results do extend to a time-varying network scenario provided that the network topology is infinitely often strongly connected [64].

Remark 2: When performing a consensus step, the PHD of every involved agent is raised to a given power $\pi \in (0, 1)$, where π is a consensus weight; unfortunately, the result of this operation cannot be computed in closed form when the PHD is represented as a GM. In practice, there are many approximation strategies, e.g. the simple strategy of [46] when GCs are well separated, or the more accurate sigma-point-based approximation [66] to be used in the case of closely spaced GCs.

V. Distributed Multivehicle SLAM

In this section, the proposed DMV-PHD-SLAM algorithm is introduced. First of all, the main working hypotheses of the considered scenario are given as follows.

1) The environment is explored by a vehicle set $\mathcal{N}$, where $|\mathcal{N}| = N$.
2) Each vehicle expresses the map in a common reference frame (or, equivalently, the transformations between the local coordinates of vehicles are exactly known).
3) Communication between two vehicles can occur depending on the relative poses of the vehicles and is modeled by means of a multivehicle network $(\mathcal{N}, \mathcal{A}_t)$ with time-varying arc set $\mathcal{A}_t$. Accordingly, the neighbors of vehicle $r \in \mathcal{N}$ are denoted as $\mathcal{N}^r_t$. It is also assumed that $\mathcal{A}_t$ (and thus $\mathcal{N}^r_t$) remain unchanged within the tth sampling interval.
4) There is no fusion center, and the vehicles are unaware of the network topology.

Note that the network arc set $\mathcal{A}_t$ is time varying as a consequence of the vehicle motion. Note also that hypothesis 2) is satisfied whenever, at the beginning of the exploration task, the relationship between the initial poses is known. This also ensures that the error on the relative poses remains bounded as long as the error with respect to the common reference remains bounded. In the case that the relative initial poses among vehicles are unknown, *registration* could be performed in advance of MV-SLAM. For this, the coordination step proposed in [25] provides a potential solution. Furthermore, in our previous work [67], [68], the problem of distributed sensor registration has been thoroughly studied in the context of multitarget tracking, and recently, the method has been extended to handle the problem of distributed multivehicle registration and mapping [69], which can be directly adopted in advance of DMV-PHD-SLAM by letting vehicles explore the same environment in order to achieve the relative initial poses, like [25] does. Since the main focus of this article is on DMV-PHD-SLAM under limited vehicle FoV, the registration issue is not addressed here.

Let x^r_t denote the pose of vehicle $r \in \mathcal{N}$ at time t, and $x^r_{0:t}$ its trajectory. Moreover, let $x^{1:N}_{0:t} = \{x^1_{0:t}, \dots, x^N_{0:t}\}$ be the collective trajectory of the vehicle team up to time t and $\mathcal{Z}^{1:N}_{1:t} = \{\mathcal{Z}^1_{1:t}, \dots, \mathcal{Z}^N_{1:t}\}$, $u^{1:N}_{0:t-1} = \{u^1_{0:t-1}, \dots, u^N_{t-1}\}$, $x^{1:N}_0 = \{x^1_0, \dots, x^N_0\}$ be defined in a similar way. Then, from a Bayesian perspective, the MV-SLAM problem amounts to the computation of the JP

$$p_{t|t}(\mathcal{M}_t, x^{1:N}_{0:t}) \triangleq p(\mathcal{M}_t, x^{1:N}_{0:t} | \mathcal{Z}^{1:N}_{0:t}, u^{1:N}_{0:t-1}, x^{1:N}_0) \tag{21}$$

which can be factorized similarly to the single-vehicle case, as follows:

$$p_{t|t}(\mathcal{M}_t, x^{1:N}_{0:t}) = p_{t|t}(x^{1:N}_{0:t})\, p_{t|t}(\mathcal{M}_t | x^{1:N}_{0:t}) \tag{22}$$

where the notation $p_{t|t}(\cdot)$ stands for the conditioning on the measurement history of all vehicles. Contrary to the centralized approach of [70], in which PHD-SLAM is extended to a multivehicle setting by employing the multisensor PHD filter [71] for the propagation of $p_{t|t}(\mathcal{M}_t | x^{1:N}_{0:t})$, in this work, a distributed approximation is obtained by making each vehicle perform single-vehicle PHD-SLAM and then, at suitable time instances, combine its map estimate with those received from the neighbors, according to the Kullback–Leibler paradigm illustrated in Section IV. It can be immediately realized that the received information will also affect the trajectory estimate via the reweighting step of the PF (step 4 in Table 1).

In order to present the proposed approach, some notation is first extended from the single-vehicle to the multivehicle SLAM scenario, as follows.

1) For each vehicle $r \in \mathcal{N}$, let M_r be the number of particles employed in the local PHD-SLAM filter, and let $\mathcal{P}^r_t$ be the set of such particles

$$\mathcal{P}^r_t = \{\mathcal{P}^{r,i}_t\}^{M_r}_{i=1}. \tag{23}$$

Authorized licensed use limited to: Universita degli Studi di Firenze. Downloaded on January 27,2025 at 10:15:12 UTC from IEEE Xplore. Restrictions apply.

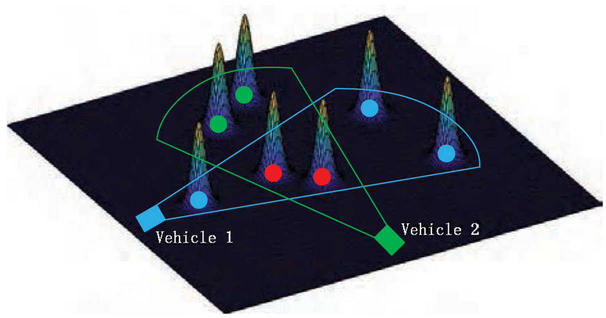

Fig. 2. Example of two-vehicle SLAM with different FoVs.

Recall that each particle consists of an importance weight $w_t^{r,i}$, a trajectory hypothesis $\widehat{x}_{0:t}^{r,i}$, and the conditional map PHD $D_{t|t}^{r,i}(\cdot|\widehat{x}_{0:t}^{r,i})$ (abbreviated as $D_{t|t}^{r,i}(\cdot)$), i.e.,

$$\mathcal{P}_t^{r,i} = \{w_t^{r,i},\, \widehat{x}_{0:t}^{r,i},\, D_{t|t}^{r,i}(\cdot)\}. \tag{24}$$

2) Let $D_{t,\ell}^{r,i}(\cdot)$ and $\widehat{D}_{t,\ell}^{r}(\cdot)$, respectively, denote the ith conditional PHD and the unconditional PHD (obtained according to either an EAP or MAP criterion) of vehicle r, at time t, after ℓ consensus iterations. Moreover, L will denote the total number of consensus iterations to be performed.
3) Let $\mathcal{V}_t^r$ denote the FoV of vehicle $r \in \mathcal{N}$ at time t.

A. Dealing With Different FoVs

In a typical MV-SLAM scenario, each vehicle is able to detect only the landmarks within its own limited FoV, as shown, for instance, in the two-vehicle scenario of Fig. 2. After an iteration of SLAM, each vehicle constructs the map PHD of the region that it has visited. If GCI fusion is adopted directly, the map PHD outside the common visited region tends to become null owing to the multiplicative nature of such a fusion rule. This means that special care has to be taken when applying the fusion strategy of (18) in order to avoid undesirable effects.

This point can be easily understood by analyzing what would be the effect of directly applying the fusion strategy of (18) to the original PHD-SLAM, as introduced in Section III-C. Recall that in the original PHD-SLAM, the initial PHD of each vehicle is equal to zero everywhere, and new GCs are initialized from the measurements after each correction step. As a result, after the first correction/birth step, the PHD of each vehicle $\widehat{D}_{1|0}^r(m)$ turns out to be nearly zero outside its own FoV $\mathcal{V}_0^r$. Then, if we consider landmarks located inside the exclusive FoVs of the vehicles (i.e., the blue and green circles in Fig. 2), the fused PHD

$$\bar{D}_{1|0}(m) = \left[\prod_{r\in\mathcal{N}} \widehat{D}_{1|0}^r(m)\right]^{\frac{1}{N}} \tag{25}$$

would be nearly zero in the neighborhood of such landmarks. As a result, no landmark would be detected when the FoVs of all vehicles are mutually disjoint. This happens because, at a basic level, the fusion strategy (18) can be interpreted as performing an *intersection* among the landmarks of different maps.

The undesirable behavior described above is essentially due to the fact that each vehicle can only initialize tracks within its own FoV. Then, in order to avoid this drawback, the idea is to modify the birth process so that each vehicle could initialize tracks also outside its own FoV on the basis of the information coming from other vehicles. Specifically, the birth process is designed so that, after each birth step, the local prediction step at time t relative to vehicle r and trajectory hypothesis i can be decomposed as

$$D_{t|t-1}^{r,i}(m) = G_{t|t-1}^{r,i}(m) + \Delta \tag{26}$$

where $G_{t|t-1}^{r,i}(m)$ is a GM containing all the information on the landmarks, while $\Delta > 0$ is a suitable constant. The constant Δ is a preset value that can be interpreted as the expected number of landmarks per unit volume of the map space. The role of the uniform component Δ in the PHD is twofold: 1) it allows each vehicle to initialize new GCs from those of the other vehicles in the fusion step; and 2) it allows each vehicle to initialize new GCs from the measurements in the correction step. This idea makes it possible to extend the usual ABM (which is also based on a uniform birth process) to the case of vehicles having different FoVs. As a result, the map PHD outside the common FoV can be preserved under the standard GCI fusion rule (18). As will be discussed in detail in Section VI, a predicted PHD of the form (26) can be obtained by means of the birth process

$$B_t^{r,i}(m) = \begin{cases} \Delta, & \text{if } t = 0 \\ \Delta \cdot P_D(m|\widehat{x}_{t-1}^{r,i}), & \text{for } t = 1, 2, \ldots \end{cases}. \tag{27}$$

This means that the initial birth density (representing the prior knowledge on the map) is uniformly distributed in the whole space, thus conveying total uncertainty on the landmark positions. In contrast, the birth process at the subsequent time instants models the detection of new landmarks within the FoV.

B. DMV-PHD-SLAM Algorithm

In the proposed algorithm, a local PHD-SLAM filter is run in each vehicle by exploiting the birth PHD model (27); then, consensus is initialized, at time t and vehicle $r \in \mathcal{N}$, as

$$D_{t,0}^{r,i}(m) = D_{t|t-1}^{r,i}(m) \tag{28}$$

$$\widehat{D}_{t,0}^{r}(m) = \widehat{D}_{t|t-1}^{r}(m). \tag{29}$$

Then, the ℓth consensus iteration takes the form

$$D_{t,\ell}^{r,i}(m) = \left[D_{t,\ell-1}^{r,i}(m)\right]^{\pi_t^{rr}} \prod_{s\in\mathcal{N}_t^r} \left[\widehat{D}_{t,\ell-1}^{s}(m)\right]^{\pi_t^{rs}} \tag{30}$$

so that, for each trajectory hypothesis i of vehicle r, the corresponding map $D_{t,\ell-1}^{r,i}(m)$ is fused with the maps $\widehat{D}_{t,\ell-1}^{s}(m)$ estimated by its neighbors using either the EAP or the MAP strategy. Note that the consensus weights π_t^{rs} are, in general, time varying, since the neighbor set $\mathcal{N}_t^r$ varies in time owing to the vehicle motion. Also observe that the product

$$\prod_{s\in\mathcal{N}_t^r} \left[\widehat{D}_{t,\ell-1}^{s}(m)\right]^{\pi_t^{rs}}$$

Authorized licensed use limited to: Universita degli Studi di Firenze. Downloaded on January 27,2025 at 10:15:12 UTC from IEEE Xplore. Restrictions apply.

is independent of the particle index i and, therefore, has to be computed only once. The proposed DMV-PHD-SLAM filter running in each vehicle $r \in \mathcal{N}$ is summarized in Algorithm 2. Note that for $t = 0$, the consensus steps can be omitted, since all the PHDs are uniform and equal to the initial value Δ.

The expression for the ℓth consensus step given by (30) deserves further attention. It can indeed be observed that the unconditional PHDs $\widehat{D}^{s}_{t,\ell-1}(m)$ received by the vehicle r are fused with each conditional PHD $D^{r,i}_{t,\ell-1}(m)$ and not with the unconditional estimate $\widehat{D}^{r}_{t,\ell-1}(m)$ corresponding to the rth vehicle itself. The rationale underlying this choice is that different particles should maintain different maps, since they are conditioned on different trajectories. However, if a large number of consensus iterations are carried out, the two approaches lead to the same result, as stated by the following theorem.

Theorem 1 (DMV-PHD-SLAM consensus): Let us consider the generic ℓth consensus iteration as in (30), and assume that the unconditional PHDs of all vehicles are estimated with the MAP criterion, at each time and consensus step. Then, for all $r \in \mathcal{N}$ and $m \in \mathbb{M}$, the following results hold.

1) The local map estimates $\widehat{D}^{r}_{t,\ell}(\cdot)$ obey the usual consensus recursion

$$\widehat{D}^{r}_{t,\ell}(m) = \prod_{s \in \mathcal{N}^r_t \bigcup \{r\}} \left[\widehat{D}^{s}_{t,\ell-1}(m)\right]^{\pi^{rs}_t}. \tag{31}$$

Consequently, under the standard assumptions of Section IV, such local estimates converge to the overall KLA of the initial map estimates as the number of consensus steps approaches infinity.

2) As $\ell \to \infty$, each particle conditional PHD converges to the overall KLA of the initial map estimates, i.e.,

$$\lim_{\ell \to \infty} D^{r,i}_{t,\ell}(m) = \bar{D}_t(m) \tag{32}$$

where $\bar{D}_t$ is the overall KLA given by

$$\bar{D}_t(m) = \left[\prod_{r \in \mathcal{N}} \widehat{D}^{r}_{t,0}(m)\right]^{\frac{1}{N}}. \tag{33}$$

Proof: See Appendix B.

Remark 3: Note that the convergence of Theorem 1 refers to the static case, i.e., when an infinite number of consensus steps are performed without any intermediate map update owing to the new measurements. Since in practice consensus steps are always alternated with measurement-based updates, the diversity between the particle maps is preserved. However, since in the limit all particles will retain the same map PHD, an alternative way of operating could be to simply perform consensus over the local estimates, as in (31) and then set

$$D^{r,i}_{t,\ell}(m) = \widehat{D}^{r}_{t,\ell}(m), \text{ for } i \in \{1, 2, \ldots, M_r\}. \tag{34}$$

Intuitively, it can be observed that such a choice would not ruin the mechanism on which the PHD-SLAM is based. Indeed, after the fusion, all the particles will share the same PHD, and such a PHD will be close to the true map, since it originates from the fusion of the (MAP or EAP) estimates. A particle

Algorithm 2: DMV-PHD-SLAM Algorithm (at Time t, Vehicle r).

Input: $\mathcal{P}^r_{t-1}$ and $\mathcal{Z}^r_t$
Predict the conditional PHD of each particle via (14) using the birth intensity (27);
Compute the estimated PHD $\widehat{D}^{r}_{t|t-1}$ from $\{D^{r,i}_{t|t-1}\}^{M_r}_{i=1}$ according to either the MAP or EAP criterion;
Initialize the consensus iterations via (28)-(29);
for $\ell = 1, \ldots, L$ **do**
  Broadcast $\widehat{D}^{r}_{t,\ell-1}$ and receive $\widehat{D}^{s}_{t,\ell-1}$, $s \in \mathcal{N}^r_t$;
  for $i = 1, \ldots, M_r$ **do**
    Fuse the conditional PHD of particle i via (30);
  end
  Compute the estimated PHD $\widehat{D}^{r}_{t,\ell}$ from $\{D^{r,i}_{t,\ell}\}^{M_r}_{i=1}$ according to either the MAP or EAP criterion;
end
Let $D^{r,i}_{t|t-1} = D^{r,i}_{t,L}$, for $i = 1, \ldots, M_r$;
Carry out steps 2-8 of Algorithm 1 to get the local posterior particle set $\mathcal{P}^{r,i}_t$;
Output: $\mathcal{P}^r_t$, $\widehat{x}^r_{t|t}$ and $\widehat{\mathcal{M}}^r_t$

whose pose hypothesis is far from ground truth will find that the measurement set acquired at the next time step does not match such a PHD and will, therefore, be given a low weight at the particle weighting step. It can be observed that this approach would be much less computationally demanding, especially if a large number of particles is adopted.

VI. Implementation of the Proposed DMV-PHD-SLAM Algorithm

In the proposed DMV-PHD-SLAM algorithm, M_r particles are maintained at each vehicle, where each particle stands for a hypothesis of the vehicle trajectory and the corresponding conditional map PHD. Hereafter, an efficient implementation of the proposed DMV-PHD-SLAM algorithm is presented. We start by considering, at the generic time t, local predicted PHDs $D^{r,i}_{t|t-1}(m)$ of the form (26). Then, we discuss in detail how the PHDs are modified in the fusion and correction steps.

A. Fusion Step

In order to streamline the presentation, we consider the case in which vehicle r has only one neighbor, say vehicle s, so that the generic consensus step simplifies to

$$D^{r,i}_{t,\ell}(m) = \left[D^{r,i}_{t,\ell-1}(m)\right]^{\pi^{rr}_t} \left[\widehat{D}^{s}_{t,\ell-1}(m)\right]^{\pi^{rs}_t} \tag{35}$$

with $\pi^{rs}_t = 1 - \pi^{rr}_t$. The proposed implementation can be directly applied also in the general case of multiple neighbors by performing fusion pairwise, i.e., vehicle-by-vehicle. This strategy is also preferable from the computational viewpoint because a direct application of (30) with the proposed ABM (27) would involve a number of GCs after fusion in the order of the product of all the numbers of GCs of the involved GMs. Conversely, by performing fusion pairwise, we can keep the

Authorized licensed use limited to: Universita degli Studi di Firenze. Downloaded on January 27,2025 at 10:15:12 UTC from IEEE Xplore. Restrictions apply.

number of GCs limited by performing pruning and merging between two successive fusion steps.

Let the PHDs to be fused be decomposed as

$$D^{r,i}_{t,\ell-1}(m) = G^{r,i}_{t,\ell-1}(m) + \Delta \tag{36}$$

$$\widehat{D}^{s}_{t,\ell-1}(m) = \widehat{G}^{s}_{t,\ell-1}(m) + \Delta \tag{37}$$

where $G^{r,i}_{t,\ell-1}(m)$ and $\widehat{G}^{s}_{t,\ell-1}(m)$ are GMs. Then, (35) can be rewritten as

$$D^{r,i}_{t,\ell}(m) = \left[G^{r,i}_{t,\ell-1}(m) + \Delta\right]^{\pi^{rr}_t} \left[\widehat{G}^{s}_{t,\ell-1}(m) + \Delta\right]^{1-\pi^{rr}_t}. \tag{38}$$

The following approximations are adopted.

1) In the region of the map space $\mathbb{M}$ where both vehicles r and s have information (i.e., the two PHDs contain GCs with nearby centers), we set

$$D^{r,i}_{t,\ell}(m) \approx \left[G^{r,i}_{t,\ell-1}(m)\right]^{\pi^{rr}_t} \left[\widehat{G}^{s}_{t,\ell-1}(m)\right]^{1-\pi^{rr}_t} + \Delta\,. \tag{39}$$

Note that the above approximation is actually exact when $G^{r,i}_{t,\ell-1}(m) = \widehat{G}^{s}_{t,\ell-1}(m)$.

2) In the region of the map space $\mathbb{M}$ where only vehicle r has information, so that $\widehat{G}^{s}_{t,\ell-1}(m)$ is nearly zero, we set

$$D^{r,i}_{t,\ell}(m) \approx \left[G^{r,i}_{t,\ell-1}(m)\right]^{\pi^{rr}_t} \Delta^{1-\pi^{rr}_t} + \Delta\,. \tag{40}$$

3) In the region of the map space $\mathbb{M}$ where only vehicle s has information, so that $G^{r,i}_{t,\ell-1}(m)$ is nearly zero, we set

$$D^{r,i}_{t,\ell}(m) \approx \Delta^{\pi^{rr}_t} \left[\widehat{G}^{s}_{t,\ell-1}(m)\right]^{1-\pi^{rr}_t} + \Delta\,. \tag{41}$$

4) In the region of the map space $\mathbb{M}$ where neither of vehicles has information, we set

$$D^{r,i}_{t,\ell}(m) \approx \Delta\,. \tag{42}$$

Based on the above considerations, an efficient GM implementation of the fusion step of the DMV-PHD-SLAM algorithm can be devised. Without loss of generality (recall Remark 2), let the powered GMs in (39)–(41) be represented in GM form as

$$\left[G^{r,i}_{t,\ell-1}(m)\right]^{\pi^{rr}_t} = \sum_{k=1}^{J^{r,i}_{t,\ell-1}} \alpha^{r,i,k}_{t,\ell-1} \mathcal{G}\left(m; \widehat{m}^{r,i,k}_{t,\ell-1}, P^{r,i,k}_{t,\ell-1}\right) \tag{43}$$

$$\left[\widehat{G}^{s}_{t,\ell-1}(m)\right]^{1-\pi^{rr}_t} = \sum_{k=1}^{J^{s}_{t,\ell-1}} \alpha^{s,k}_{t,\ell-1} \mathcal{G}\left(m; \widehat{m}^{s,k}_{t,\ell-1}, P^{s,k}_{t,\ell-1}\right). \tag{44}$$

Note that in the GM representations (43) and (44), each GC stands for a potential landmark. If the kth GC of $D^{r,i}_{t,\ell-1}$ is close to the nth GC of $D^{s}_{t,\ell-1}$, both GCs belong to case 1 above. Conversely, if the kth GC of $D^{r,i}_{t,\ell-1}$ is not close to any GC of $D^{s}_{t,\ell-1}$, then it belongs to case 2.

Accordingly, the problem of interest becomes to check for every GC of vehicle r, whether another GC of the neighboring vehicle s can be associated with it. This can be accomplished by resorting to a gating method [72]. Specifically, the kth GC of vehicle r is associated with the nth GC of vehicle s whenever $T^{kn}_{t,\ell-1} \le T_\omega$, where

$$T^{kn}_{t,\ell-1} = \left(\widehat{m}^{r,i,k}_{t,\ell-1} - \widehat{m}^{s,n}_{t,\ell-1}\right)^\top \left(P^{r,i,k}_{t,\ell-1} + P^{s,n}_{t,\ell-1}\right)^{-1} \times \left(\widehat{m}^{r,i,k}_{t,\ell-1} - \widehat{m}^{s,n}_{t,\ell-1}\right) \tag{45}$$

is the Mahalanobis distance between the two GCs and T_ω a preset threshold. As a result, one can find two index sets representing the respective GCs that can or cannot be matched to each other (denoted as $M^{r,A,i}_{t,\ell-1}$, $M^{s,A}_{t,\ell-1}$ and $M^{r,L,i}_{t,\ell-1}$, $M^{s,L}_{t,\ell-1}$, respectively). Then, the fused PHD takes again the form

$$D^{r,i}_{t,\ell}(m) = G^{r,i}_{t,\ell}(m) + \Delta \tag{46}$$

where $G^{r,i}_{t,\ell}(m)$ is a GM computed as follows:

$$\begin{aligned} G^{r,i}_{t,\ell}(m) = &\sum_{k\in M^{r,A,i}_{t,\ell-1}} \sum_{n\in M^{s,A}_{t,\ell-1}} \alpha^{r,i,k}_{t,\ell-1}\alpha^{s,n}_{t,\ell-1} \mathcal{G}\left(m; \widehat{m}^{r,i,k}_{t,\ell-1}, P^{r,i,k}_{t,\ell-1}\right) \\ &\times \mathcal{G}\left(m; \widehat{m}^{s,n}_{t,\ell-1}, P^{s,n}_{t,\ell-1}\right) \\ &+ \Delta^{1-\pi^{rr}_t} \sum_{k\in M^{r,L,i}_{t,\ell-1}} \alpha^{r,i,k}_{t,\ell-1} \mathcal{G}\left(m; \widehat{m}^{r,i,k}_{t,\ell-1}, P^{r,i,k}_{t,\ell-1}\right) \\ &+ \Delta^{\pi^{rr}_t} \sum_{n\in M^{s,L}_{t,\ell-1}} \alpha^{s,n}_{t,\ell-1} \mathcal{G}\left(m; \widehat{m}^{s,n}_{t,\ell-1}, P^{s,n}_{t,\ell-1}\right) \end{aligned} \tag{47}$$

The proposed method for efficiently fusing map GM-PHDs of two vehicles with different FoVs is detailed in Algorithm 3. The following remark discusses how to substantially reduce the algorithm's computational load by avoiding unnecessary fusions.

Remark 4: Because of the limitation of sensor FoV, a vehicle can only explore a small region of the environment at each time instance. Hence, the detected landmarks (represented by GCs) located outside the collective FoV of the robots involved in fusion remain unchanged. Since the fusion has been performed in previous recursions and the states of these landmarks have reached consensus, it is not necessary to perform GCI fusion on such landmarks (GCs) even though they are matched at the current time instance. Under this consideration, another check should also be performed to find the matched landmark pairs, whose Mahalanobis distance $T^{kn}_{t,\ell-1}$ is sufficiently close to zero, and then these landmarks are directly copied into the fused PHD in order to save computations.

B. Correction and Prediction

Let us now focus on the correction step and consider application of the PHD update equation (16) to a predicted density $D^{r,i}_{t|t-1} = D^{r,i}_{t,L}$ of the form (26). As discussed in the previous section, this can be done without loss of generality, since the form (26) is preserved under fusion. Then, for each vehicle r

Authorized licensed use limited to: Universita degli Studi di Firenze. Downloaded on January 27,2025 at 10:15:12 UTC from IEEE Xplore. Restrictions apply.

Algorithm 3: Fusion of PHDs With Different FoVs Between Vehicles r and s.

Input: $D^{r,i}_{t,\ell-1}(m)$ $(i=1,\ldots,M_r)$, $\widehat{D}^{s}_{t,\ell-1}(m)$ and T_ω

Initialize empty index sets $M^{r,A,i}_{t,\ell-1}=\emptyset$, $M^{r,L,i}_{t,\ell-1}=\emptyset$, $M^{s,A}_{t,\ell-1}=\emptyset$, and $M^{s,L}_{t,\ell-1}=\emptyset$;
for $k=1,\ldots,J^{r,i}_{t,\ell-1}$ **do**
  for $n=1,\ldots,J^{s}_{t,\ell-1}$ **do**
    Compute $T^{kn}_{t,\ell-1}$ according to (45);
    if $T^{kn}_{t,\ell-1}\le T_\omega$ **then**
      Add k into $M^{r,A,i}_{t,\ell-1}$, and add n into $M^{s,A}_{t,\ell-1}$;
    end
  end
end
Set $M^{r,L,i}_{t,\ell-1}$ and $M^{s,L}_{t,\ell-1}$ as
$M^{r,L,i}_{t,\ell-1}=\left\{1,\ldots,J^{r,i}_{t,\ell-1}\right\}\setminus M^{r,A,i}_{t,\ell-1}$ and
$M^{s,L}_{t,\ell-1}=\left\{1,\ldots,J^{s}_{t,\ell-1}\right\}\setminus M^{s,A}_{t,\ell-1}$;
Compute the fused PHD $D^{r,i}_{t,\ell}(m)$ according to (46)-(47) .

Output: $D^{r,i}_{t,\ell}(m)$ $(i=1,\ldots,M_r)$

and each trajectory hypothesis i, the updated PHD will take the form

$$D^{r,i}_{t|t}(m)=\left[1-P_D(m|\hat{x}^{r,i}_t)\right]\left[G^{r,i}_{t|t-1}(m)+\Delta\right]+\sum_{z\in\mathcal{Z}^r_t}\Psi^{r,i}_t(z|m)\left[G^{r,i}_{t|t-1}(m)+\Delta\right] \tag{48}$$

where

$$\Psi^{r,i}_t(z|m)=\frac{P_D(m|\hat{x}^{r,i}_t)g^r_t(z|m,\hat{x}^{r,i}_t)}{\kappa^r(z|\hat{x}^{r,i}_t)+\int P_D(m|\hat{x}^{r,i}_t)g^r_t(z|m,\hat{x}^{r,i}_t)\left[G^{r,i}_{t|t-1}(m)+\Delta\right]dm}. \tag{49}$$

Note that the updated PHD contains the following four terms.

a) The term $[1-P_D(m|\hat{x}^{r,i}_t)]\,G^{r,i}_{t|t-1}(m)$ preserves the predicted GCs with weight decreasing with the detection probability. For instance, outside the FoV where $P_D(m|\hat{x}^{r,i}_t)=0$ and hence landmarks cannot be detected, the GCs are not modified.

b) The term $\sum_{z\in\mathcal{Z}^r_t}\Psi^{r,i}_t(z|m)\,G^{r,i}_{t|t-1}(m)$ updates the predicted GCs on the basis of the collected measurements.

c) The term $\sum_{z\in\mathcal{Z}^r_t}\Psi^{r,i}_t(z|m)\,\Delta$ generates new GCs from the measurements in order to account for newly-appeared or previously undetected landmarks. This term is analogous to the so-called ABM [48], [49].

d) The term $[1-P_D(m|\hat{x}^{r,i}_t)]\,\Delta$ does not contain any information on the landmarks and simply plays the role of preserving the uncertainty on the map outside the FoV.

Terms a)–c) can be effectively approximated as GMs. The interested reader is referred to [48] and [49] for details on the GM approximation of the correction step with ABM. Summing up, after the correction step, the updated PHD can be written as

$$D^{r,i}_{t|t}(m)=G^{r,i}_{t|t}(m)+[1-P_D(m|\hat{x}^{r,i}_t)]\,\Delta \tag{50}$$

where $G^{r,i}_{t|t}(m)$ is the GM approximating terms a)–c). Finally, this updated PHD becomes the predicted PHD at time $t+1$ by means of the birth process (27), so that

$$D^{r,i}_{t+1|t}(m)=G^{r,i}_{t|t}(m)+\Delta\,. \tag{51}$$

Note that, as a matter of fact, term d) need not be computed, since it does not contain any information on the landmarks, and since only the predicted PHD $D^{r,i}_{t+1|t}(m)$ is used in the fusion step at time $t+1$.

C. Complexity Analysis

Since the expected number of landmarks per unit volume Δ is a preset constant value, the *correction and prediction* steps in Section VI-B are the same as in the standard PHD-SLAM algorithm [18]–[22]. Furthermore, the contribution of this article concerns the *fusion* step, and, accordingly, the complexity analysis will focus only on this step.

In the pairwise fusion presented in Section VI-A, fusion only involves two map PHDs. It can be seen immediately from (47) that the fusion of two map PHDs of vehicles r and s has complexity

$$O(|M^{r,A,i}_{t,\ell-1}|\cdot|M^{s,A}_{t,\ell-1}|)+O(|M^{r,L,i}_{t,\ell-1}|)+O(|M^{s,L}_{t,\ell-1}|) \tag{52}$$

where $O(\cdot)$ stands for "*in the order of.*" When performing DMV-PHD-SLAM with Algorithm 2, the above computational complexity will also be multiplied by the number of particles M_r. This actually represents the maximum computational complexity when the proposed map fusion strategy is performed. In practice, such complexity can be significantly reduced by adopting the strategies of Remarks 3 and 4.

When the fusion involves more than two vehicles, in principle, the number of matched GCs increases with the number of vehicles, so that a direct application of (30) would involve

$$O\left(\sum_{\mathcal{S}\subseteq\bar{\mathcal{N}}^r_t}\prod_{s\in\mathcal{S}}|M^{s,A}_{\mathcal{S}}|\right) \tag{53}$$

operations, where $\bar{\mathcal{N}}^r_t=\{r\}\cup\mathcal{N}^r_t$, and for any subset $\mathcal{S}\subseteq\bar{\mathcal{N}}^r_t$ of vehicles, $M^{s,A}_{\mathcal{S}}$ denotes the subset of GCs of vehicle $s\in\mathcal{S}$ matched to all other vehicles in $\mathcal{S}$. However, as anticipated, when fusion is performed pairwise, the computational complexity can be significantly reduced by applying the pruning and merging methods between successive fusion steps so as to reduce the number of GCs. Furthermore, inherited from the consensus broadcasting protocol (see [46, Sec. III]), the complexity of the proposed DMV-PHD-SLAM algorithm running in each vehicle is related to the number of neighbors rather than the whole size of the vehicle network. Hence, it is immediately seen that the proposed DMV-PHD-SLAM algorithm is scalable with respect to the number of involved vehicles.

Authorized licensed use limited to: Universita degli Studi di Firenze. Downloaded on January 27,2025 at 10:15:12 UTC from IEEE Xplore. Restrictions apply.

In the particle representation (24), each particle consists of a scalar particle weight, a vehicle trajectory, and a conditional PHD. As pointed out in Section VI-A, each GC of the GM represents a potential landmark. Hence, in the ideal case, each particle contains $1 + (t+1) \times \dim(x) + |\mathcal{M}_t| \times [1+\dim(m)][1+\frac{\dim(m)}{2}]$ real numbers at time t (since the covariance matrix of each GC is symmetrical and the trajectory of each vehicle is recorded from $t = 0$), where $\dim(\cdot)$ stands for vector dimension. Compared to the traditional RBPF-based method (e.g., FastSLAM [9]) that records, for each particle, the particle weight, vehicle trajectory, mean vector, and covariance matrix of each landmark, the proposed method will have to record $|\mathcal{M}_t|$ more real numbers for each particle, corresponding to the weights of each GC.

Remark 5: As far as fusion is performed, each vehicle can get access to the landmarks outside its explored region, which essentially increase the number of detected landmarks compared to local SLAM. As a result, the computational load of *correction and prediction* steps as well as memory occupation in each vehicle will increase. Certainly, such sacrifice is worth, since a global map can be built at each vehicle and can also help to improve its localization accuracy.

VII. Performance Evaluation

In this section, the proposed DMV-PHD-SLAM algorithm is evaluated via both simulations and the two experimental mapping datasets of UTIAS [50] and Victoria park[2] [51]. In all cases, landmarks are motionless and located within a planar region, i.e., represented as $m = [\bar{\xi}\ \bar{\eta}]^\top$, where $\bar{\xi}$ and $\bar{\eta}$ denote horizontal and vertical Cartesian coordinate of position, respectively. The pose of each mobile robot is represented by the 3-D state vector $x = [\xi\ \eta\ \theta]^\top$, where ξ and η specify the position of the vehicle, while θ is the orientation angle relative to the horizontal axis. Moreover, the control variable at time t is described as $u_t = [\delta_t\ \Omega_t]^\top$, where δ_t denotes the robot speed and Ω_t the angular velocity. In this section, two different types of motion model (1) are considered for each vehicle r depending on the experiments. Specifically, we have the following.

1) For the simulation and UTIAS datasets, the motion model (1) of robot r is given by [6]

$$x_t^r = f_t\left(x_{t-1}^r, u_{t-1}^r, w_t^r\right) = x_{t-1}^r + \begin{bmatrix} T\cdot\cos\theta_{t-1}^r & 0 \\ T\cdot\sin\theta_{t-1}^r & 0 \\ 0 & T \end{bmatrix}\left(u_{t-1}^r + w_t^r\right) \tag{54}$$

where the process noise w_t^r is normally distributed with zero mean and covariance $Q_t = \mathrm{diag}(\sigma_\delta^2, \sigma_\Omega^2)$.

2) For the Victoria park dataset, the motion model (1) of robot r is given by

$$x_t^r = f_t\left(x_{t-1}^r, u_{t-1}^r, w_t^r\right) = x_{t-1}^r + \begin{bmatrix} V_{t-1}^r\cdot\left(T\cdot\cos(\theta_{t-1}^r) - \frac{\psi_{t-1}^r\cdot\tan(\Omega_{t-1}^r)}{H_2}\right) \\ V_{t-1}^r\cdot\left(T\cdot\sin(\theta_{t-1}^r) + \frac{\varphi_{t-1}^r\cdot\tan(\Omega_{t-1}^r)}{H_2}\right) \\ T\cdot\frac{V_{t-1}^r}{H_2}\cdot\tan\left(\Omega_{t-1}^r\right) \end{bmatrix} + w_t^r \tag{55}$$

where

$$V_{t-1}^r = \frac{\delta_{t-1}^r}{\left[1-\tan\left(\Omega_{t-1}^r\right)\cdot\frac{H_1}{H_2}\right]} \tag{56}$$

$$\psi_{t-1}^r = a\cdot\sin(\theta_{t-1}^r) + b\cdot\cos(\theta_{t-1}^r) \tag{57}$$

$$\varphi_{t-1}^r = a\cdot\cos(\theta_{t-1}^r) - b\cdot\sin(\theta_{t-1}^r) \tag{58}$$

and the vehicle-related parameters are set to $H_1 = 0.76$ m, $H_2 = 2.83$ m, $a = 3.78$ m, and $b = 0.5$. In this case, the process noise w_t^r is taken as white Gaussian with zero mean and covariance $Q_t = \mathrm{diag}(\sigma_\xi^2, \sigma_\eta^2, \sigma_\theta^2)$.

Furthermore, in all cases, the sensors onboard each vehicle provide the relative angle and distance between the detected landmark and the vehicle, so that the measurement function is given by

$$h\left(m, x_t^r\right) = \begin{bmatrix} \sqrt{\left(\bar{\xi}-\xi_t^r\right)^2 + \left(\bar{\eta}-\eta_t^r\right)^2} \\ \mathrm{atan2}(\bar{\xi}-\xi_t^r, \bar{\eta}-\eta_t^r) - \theta_t^r \end{bmatrix} \tag{59}$$

where atan2 denotes the four quadrant inverse tangent.[3] The measurement noise is supposed to be normally distributed with zero mean and covariance $R_t = \mathrm{diag}(\sigma_d^2, \sigma_\phi^2)$. Accordingly, the single-object likelihood function $g_t^r(z|m, x_t)$ is given by

$$g_t\left(z|\, m, x_t^r\right) = \mathcal{G}\left(z; h\left(m, x_t^r\right), R_t\right). \tag{60}$$

Two performance indicators are considered, namely the *average mean square error* (AMSE), which quantifies the accuracy of vehicle localization, and the *optimal subpattern assignment* (OSPA) distance [77], [78], which quantifies the accuracy of joint landmark cardinality and position error between the estimated map RFS and the ground-truth one. In particular, we have the following.

1) The ground-truth map RFS at time t consists of all landmarks that have been in the FoV of some robot $r \in \mathcal{N}$ at some time $k \le t$;
2) The estimated map RFS is extracted from the unconditional PHDs $\widehat{D}_{t|t}^r(\cdot)$, $r \in \mathcal{N}$, according to the MAP criterion.

The involved algorithms are programmed based on MATLAB 2018 launched on a desktop with CPU E3-1225 at 3.30 GHz, 16-GB memory, and 64-bit Windows 10 operating system. Furthermore, in order to evaluate the communication burden,

[2]The Victoria park dataset was originally collected for SV-SLAM. In our experiment, the long-term vehicle trajectory has been manually divided into four parts, where each part has been assigned to a virtual vehicle so as to artificially produce a multivehicle scenario. The details are reported in Section VII-C.

[3]Note that, in the Victoria park dataset, the angle reference line is vertical to the vehicle so that the angle measurement function becomes $\mathrm{atan2}(\bar{\xi}-\xi_t^r, \bar{\eta}-\eta_t^r) - \theta_t^r + \frac{\pi}{2}$.

Authorized licensed use limited to: Universita degli Studi di Firenze. Downloaded on January 27,2025 at 10:15:12 UTC from IEEE Xplore. Restrictions apply.

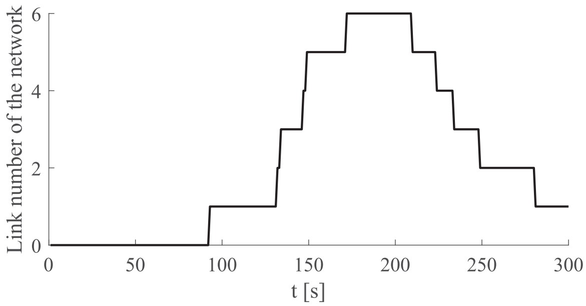

Fig. 3. Link number variation: simulated scenario.

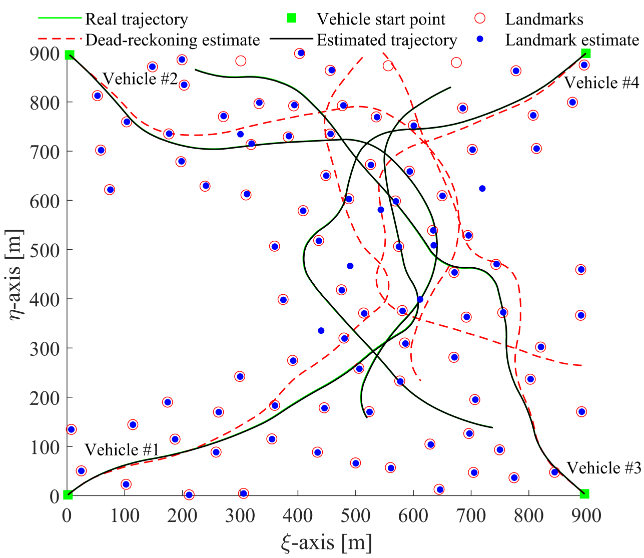

Fig. 4. Simulated scenario with the results of a typical run.

it is supposed that each real number is represented in 4-byte single-precision floating-point format.

In the real data experiments, the parameters of the considered SLAM algorithms have been tuned according to the available knowledge of the sensor characteristics (for the FoV and measurement noise variance) and to statistics on the dataset for the clutter.

A. Simulated Dataset

In the simulated scenario of Fig. 4, a team of four robots is exploring a $900 \times 900\ \mathrm{m}^2$ region, which contains 85 randomly deployed landmarks. The standard deviations of the control input are set to $\sigma_\delta = 0.025\ \mathrm{m/s}$ and $\sigma_\Omega = 0.02\ \mathrm{rad/s}$. It is also assumed that robot r exchanges data with another robot s if and only if their distance is less than $T_d = 300\ \mathrm{m}$. Note that such choice is conservative enough since there are actually communication devices that support the coverage range up to over 3 km (see [79, Table I]). The landmarks inside the FoV of each vehicle r are detected with probability $P_d^r = P_d = 0.98$, and the measurement set is renewed at every robot with sampling interval $T = 1$ s. The standard deviations of measurement noises are set to $\sigma_d = 1\ \mathrm{m}$ for range and $\sigma_\phi = \frac{0.5\pi}{180}$ rad for azimuth. The FoV of each robot changes in time and, specifically, consists of a sector of a circular annulus with angular extension $[-\frac{\pi}{2}, \frac{\pi}{2}]$ rad around the current robot orientation and range extension $[0, 150]$ m from the current robot position. The clutter intensity inside the FoV of each robot is taken as $\kappa(z) = 0.0075$ at each time t (i.e., the expected number of clutter points inside the FoV at each time is equal to 3.5, which actually represents a dense clutter scenario compared to the number of average observed landmarks per vehicle at each time, which is 4.06).

The parameters of the DMV-PHD-SLAM algorithm have been chosen as follows. For each robot r, the number of particles is set to $M_r = 100$; the threshold for distinguishing between matched and unmatched GCs is set to $T_\omega = 5$. After the end of consensus, at each time and in each robot, the resulting PHD undergoes a pruning and merging procedure with pruning threshold $T_P = 10^{-5}$ and merging threshold $T_M = 2.5$.

The link number of the time-varying vehicle network is plotted versus time in Fig. 3 (recall that the total number of possible links for a four-agent network is equal to 6). It can be seen that the vehicles start to exchange data from about 100 s, and the full connection time of the vehicle network is much smaller than the overall simulation time. The results of a typical run of the DMV-PHD-SLAM algorithm with $L = 1$ in the simulated scenario are illustrated in Fig. 4. As can be observed qualitatively, the proposed algorithm can properly accomplish the distributed multirobot SLAM task.

Next, robot localization and mapping performance are examined separately. First, Fig. 5(a) quantifies robot localization performance by means of the position AMSE, averaged over all vehicles and 100 independent Monte Carlo trials. Here, the performance of a distributed implementation of FastSLAM 2.0 (denoted as D-FastSLAM hereafter) [10] and centralized EKF-SLAM [75] (denoted as C-EKF-SLAM hereafter) is also incorporated so as to provide comparisons. More specifically, we have the following.

1) D-FastSLAM follows a distributed configuration, in which the nearest-neighbor method is exploited for measurement-to-landmark association, and for $L \geq 1$, map fusion is performed by the method in [40] with landmark association among vehicles performed via 2-D assignment [76].
2) C-EKF-SLAM follows a centralized configuration, in which the states of all vehicles and landmarks are stacked into an augmented state vector, and 2-D assignment is exploited for measurement-to-landmark association.
3) Both D-FastSLAM and C-EKF-SLAM are periodically checked every period of 5 s so as to remove false landmarks (i.e., landmarks that are detected no more than twice during this period).

Note that FastSLAM has the same structure than PHD-SLAM (i.e., both are based on RBPF), thus enjoying similar characteristics (inherited from the PF). It can be seen that the proposed DMV-PHD-SLAM algorithm provides a much better vehicle localization performance than both D-FastSLAM and C-EKF-SLAM in both local ($L = 0$) and cooperative ($L \geq 1$) SLAM. The reason of such results is that, inherited from PHD-SLAM,

Authorized licensed use limited to: Universita degli Studi di Firenze. Downloaded on January 27,2025 at 10:15:12 UTC from IEEE Xplore. Restrictions apply.

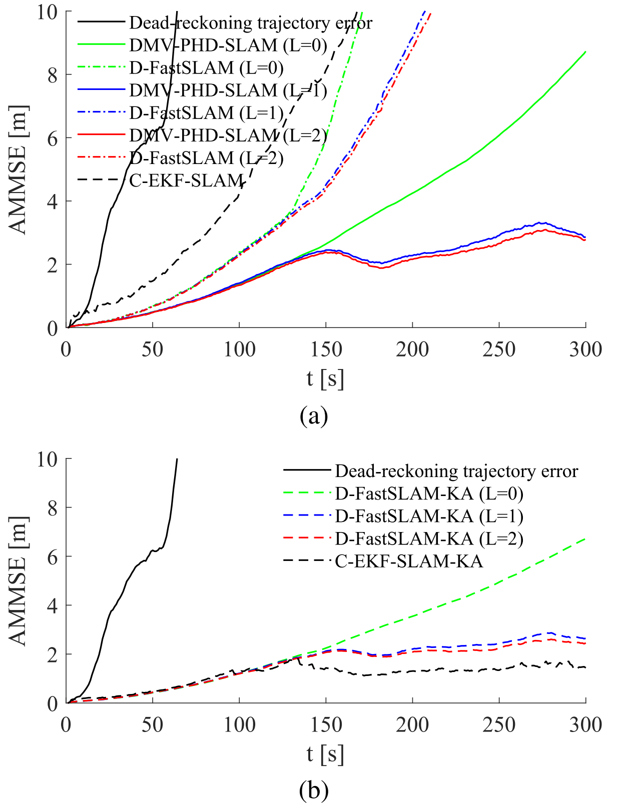

Fig. 5. Localization performance: simulation results. (a) Unknown association and clutterly measurements. (b) Known association and clutter-free measurements.

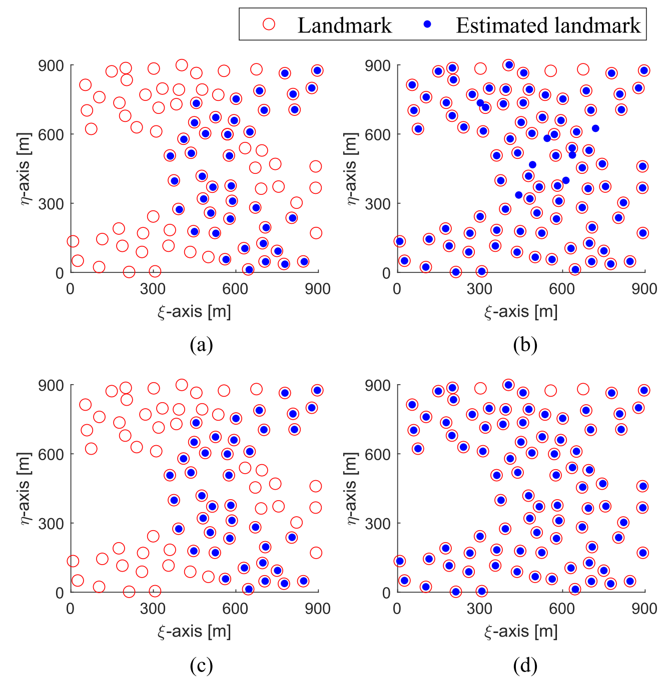

Fig. 6. Map estimation comparison among distributed SLAM algorithms. (a) DMV-PHD-SLAM with $L = 0$. (b) DMV-PHD-SLAM with $L = 1$. (c) D-FastSLAM ($L = 0$) with known association and clutter-free measurements. (d) Consensus D-FastSLAM ($L = 1$) with known association and clutter-free measurements.

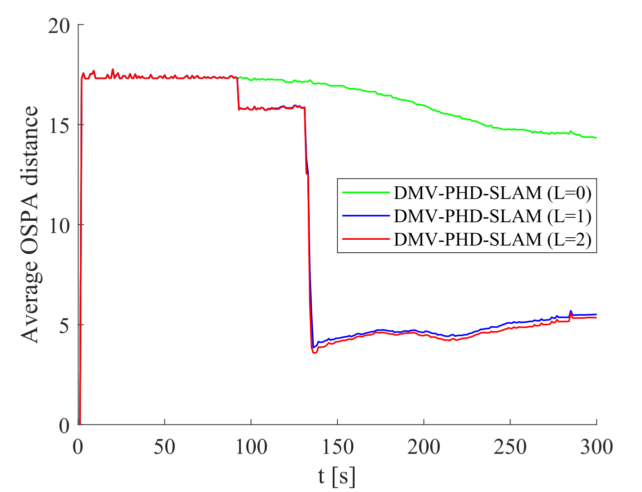

Fig. 7. Mapping performance of the DMV-PHD-SLAM algorithm: simulation results.

DMV-PHD-SLAM has advantages in dealing with (dense) clutter (as confirmed in [15], [18], and [20]). In order to better see this fact, we have also evaluated the localization performance of D-FastSLAM and C-EKF-SLAM in the simplified case of *known measurement-to-landmark association and clutter-free* measurements.[4] The results obtained in this case are reported in Fig. 5(b). Note that, here and in the following, we utilize the acronym KA (known association) to indicate results obtained in this simplified setting. A comparison of Fig. 5(a) and (b) confirms that the reasons for the divergent behavior of D-FastSLAM and C-EKF-SLAM in Fig. 5(a) are the unknown measurement-to-landmark association and the presence of clutter (false measurements), whereas DMV-PHD-SLAM is inherently designed to handle these additional sources of uncertainty. Furthermore, compared to the performance improvement from $L = 0$ to $L = 1$, slight improvements are observed for $L > 1$ consensus steps. The main reason of such result is that, since the explored environment consists only of static landmarks, the information on the landmarks can actually be diffused throughout the vehicle network also with multiple time recursions without requiring multiple consensus steps per recursion.

Next, mapping performance will be taken into consideration. For the sake of comparison, the mapping results of a typical run at robot 1 are illustrated in Fig. 6. It can be seen that the robot is able to detect more landmarks when it exchanges messages with its neighbors. Then, the OSPA map distances (with cutoff $c = 20$ and order $p = 2$), averaged over 100 Monte Carlo trials, of the proposed DMV-PHD-SLAM algorithm are illustrated in Fig. 7. Since D-FastSLAM and C-EKF-SLAM are heavily affected by clutter, their mapping performance turns out to be very poor and will not be shown hereafter. It can be seen quantitatively that mapping performance improves when robots can exchange data, thus demonstrating the effectiveness of PHD consensus. It can be observed that also mapping performance,

[4]The details of D-FastSLAM with known data association are deferred to Appendix C.

Authorized licensed use limited to: Universita degli Studi di Firenze. Downloaded on January 27,2025 at 10:15:12 UTC from IEEE Xplore. Restrictions apply.

TABLE I
AVERAGE PERFORMANCE COMPARISON (PER RECURSION)

	DMV-PHD-SLAM			DMV-PHD-SLAM-V1			D-FastSLAM			C-EKF-SLAM (Centralized)
	$L=0$	$L=1$	$L=2$	$L=0$	$L=1$	$L=2$	$L=0$	$L=1$	$L=2$	
Local SLAM computing time $[s]$	0.59	0.71	0.78	116.22	110.75	112.06	0.18	0.29	0.31	0.02
Map fusion computing time $[s]$	–	0.35	0.68	–	3.33	6.30	–	2.36	4.84	–
Vehicle localization error $[m]$	3.97	2.61	2.56	4.37	2.78	2.64	12.08	7.81	7.44	11.39
OSPA $[m]$	17.39	12.31	12.19	18.72	13.06	12.86	17.19	15.92	15.88	14.78
Communication burden [Byte]	–	1587.9	3121.5	–	3696.1	7322.6	–	2561.6	5194.7	–

like the localization one, does not significantly improve when the number of consensus steps increases.

Finally, we examine the computational and communication burden in terms of execution time and packet size, respectively. The original version of DMV-PHD-SLAM (named DMV-PHD-SLAM-V1) proposed in [47] is also considered in this comparison. In DMV-PHD-SLAM-V1, the initial map PHD (see [47, eqs. (37)–(40)]) is constructed by dividing the map space into 180 bins of size $5 \times 5\,\mathrm{m}^2$, and the scalar β in [47, eq. (40)] is chosen as $\beta = 1.8$. In the fusion part of DMV-PHD-SLAM-V1, the strategy introduced in Remark 4 is adopted. The results are reported in Table I. Note that C-EKF-SLAM, being a centralized algorithm, does not involve map fusion, and hence, its execution time in Table I is totally attributed to local SLAM; furthermore, its communication burden is not considered, since only measurements are transmitted to the fusion center.

From the examination of Table I, the following observations can be made.

1) Compared to DMV-PHD-SLAM, DMV-PHD-SLAM-V1 has significantly greater computational load, in both local SLAM and map fusion, as well as communication load owing to the much larger number of involved GCs.
2) Due to the fact that D-FastSLAM is badly affected by clutter, it has a larger average communication burden than DMV-PHD-SLAM for delivering clutter; also, due to clutter, the mapping performance of D-FastSLAM is much worse compared to DMV-PHD-SLAM.
3) C-EKF-SLAM exhibits a much smaller average execution time than the other algorithms, since it does not employ multiple particles.
4) Despite the larger computation and communication costs, the performance of vehicle localization and mapping does not improve so significantly whenever multiple consensus steps are carried out. Hence, in practice, taking into account the limited energy resources of vehicles, it is advisable to perform consensus only once per sampling interval.

B. UTIAS Dataset

In this subsection, the performance of the proposed DMV-PHD-SLAM algorithm is experimentally assessed via the UTIAS dataset [50], which has been collected through an indoor experiment. In the experiment, all landmarks and robots are tied with a unique barcode, which is used for identification. Each robot was equipped with a monocular camera, which provided images at a rate of 10 Hz. The barcodes, ranges, and bearings of the landmarks inside the FoV were directly extracted from the

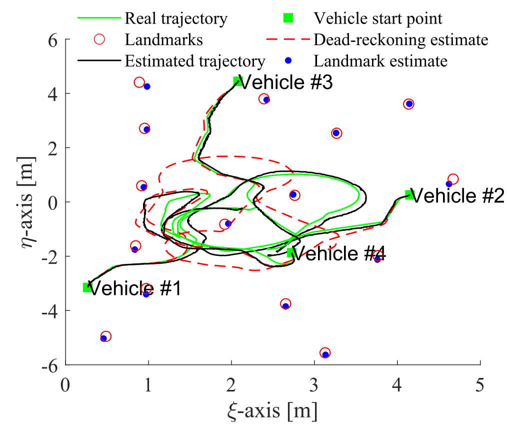

Fig. 8. Experimental UTIAS scenario: results of a typical run.

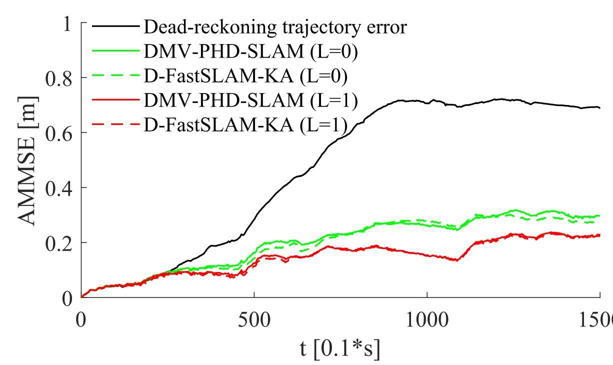

Fig. 9. Localization performance comparisons: the UTIAS dataset.

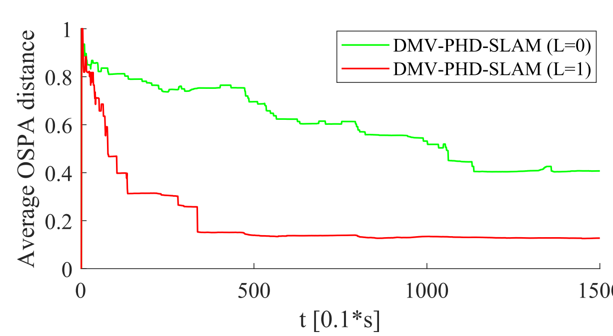

Fig. 10. Mapping performance of the DMV-PHD-SLAM algorithm: UTIAS experimental results.

images. In the experiment, the FoV extension of all robots is set to $[-0.5760\ 0.5760]\,\mathrm{rad} \times [0.8\ 8]\,\mathrm{m}$. The standard deviations of measurement noise are set to $\sigma_d = 0.5\,\mathrm{m}$ and $\sigma_\phi = 0.05\,\mathrm{rad}$,

Authorized licensed use limited to: Universita degli Studi di Firenze. Downloaded on January 27,2025 at 10:15:12 UTC from IEEE Xplore. Restrictions apply.

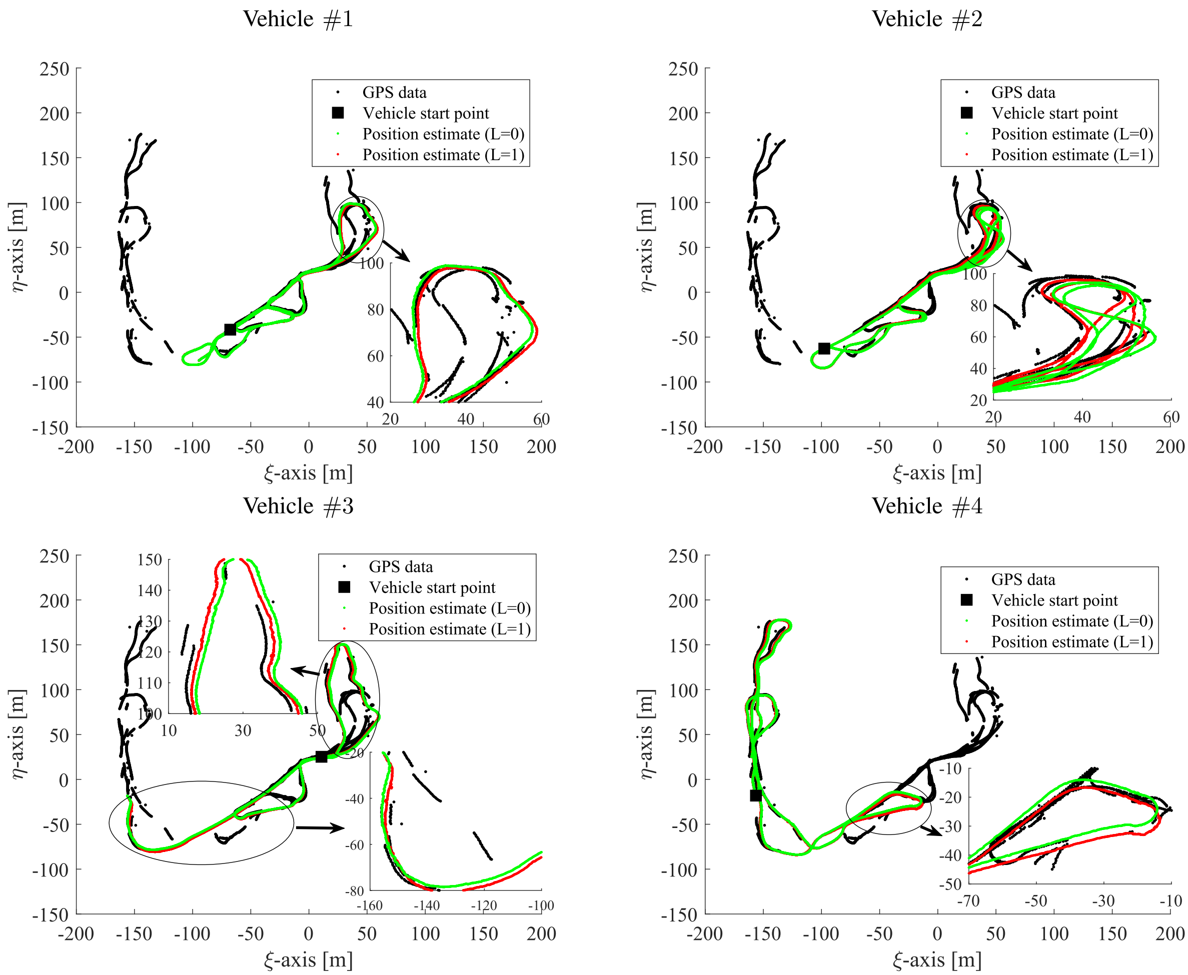

Fig. 11. Vehicle localization comparison for the Victoria park dataset. GPS data are represented by black dots, vehicle start points with black squares, and vehicle position estimates relative to $L = 0, 1$ with green and red points, respectively.

TABLE II
AVERAGE PERFORMANCE COMPARISON WITH UTIAS DATASET
(PER RECURSION)

	DMV-PHD-SLAM		D-FastSLAM-KA	
	$L=0$	$L=1$	$L=0$	$L=1$
Local SLAM computing time $[s]$	0.07	0.09	0.03	0.03
Map fusion computing time $[s]$	–	0.02	–	0.02
Vehicle localization error $[m]$	0.21	0.14	0.21	0.13
OSPA $[m]$	0.60	0.19	–	–
Communicational burden [Byte]	–	357.2	–	284.6

respectively. The standard deviations of odometry noises are set to $\sigma_\delta = 0.03\,\mathrm{m/s}$ and $\sigma_\Omega = 0.3\,\mathrm{rad/s}$, respectively.

The measurement sets of four robots have been utilized. It is assumed that two robots set up a bidirectional connection if and only if their distance is less than $T_d = 3.5\,\mathrm{m}$. The threshold for distinguishing between matched and unmatched GCs is set to $T_\omega = 0.3$; pruning and merging thresholds are set to $T_P = 10^{-5}$ and $T_M = 0.3$, respectively. A typical run of the proposed DMV-PHD-SLAM algorithm with $L = 1$ is illustrated in Fig. 8. It can be seen that distributed SLAM can be effectively accomplished.

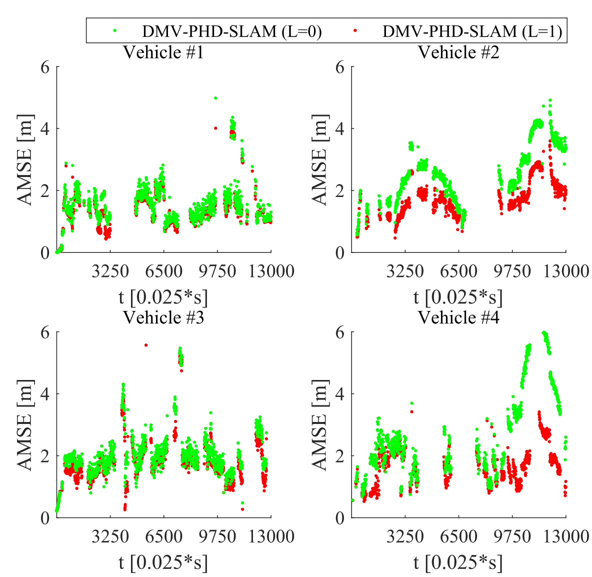

Fig. 12. Localization performance comparison: the Victoria park dataset. Local DMV-PHD-SLAM ($L = 0$) in green and cooperative DMV-PHD-SLAM ($L = 1$) in red.

Authorized licensed use limited to: Universita degli Studi di Firenze. Downloaded on January 27,2025 at 10:15:12 UTC from IEEE Xplore. Restrictions apply.

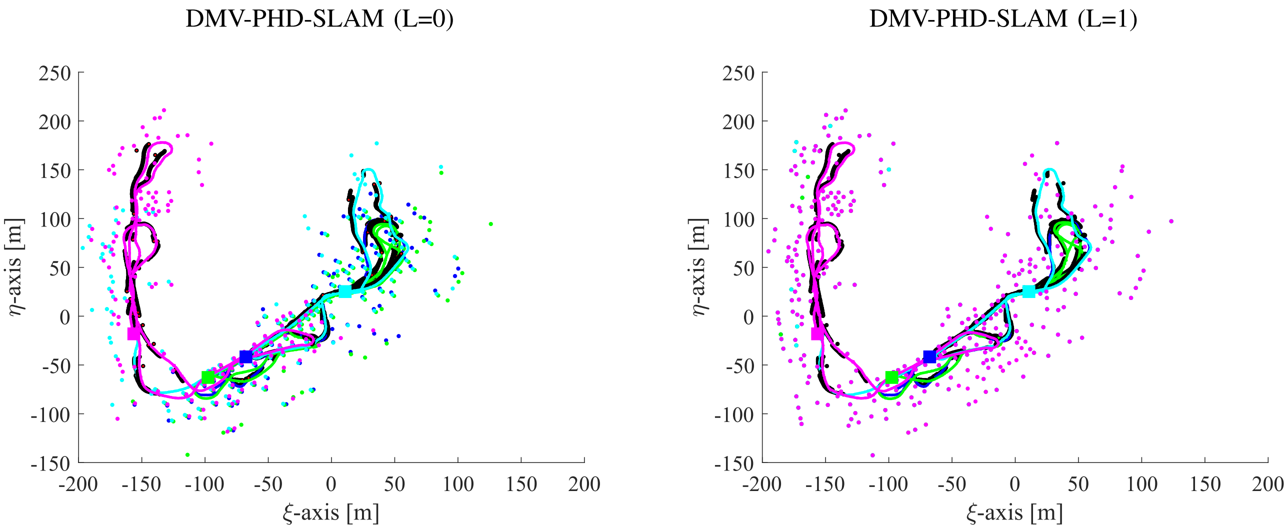

Fig. 13. Collective performance of MV-SLAM (Victoria park dataset). GPS data are represented by black dots, starting points of vehicles with black squares, the estimated vehicle trajectories are depicted with lines, and estimated landmarks are represented by dots. The SLAM results of different vehicles are distinguished with different colors.

Next, localization and mapping performance of the proposed DMV-PHD-SLAM algorithm are illustrated in Figs. 9 and 10, respectively. Note that for the UTIAS dataset, the labels of landmarks are known by extracting the barcodes tied to the landmarks and can, therefore, be exploited to avoid data association. Hence, D-FastSLAM with perfectly known measurement-to-landmark association ($L = 0$) and its consensus version ($L = 1$) are also considered as baselines for the performance achievable in the experiment. Similarly to the simulated scenario, it can be concluded that the SLAM performance significantly improves when robots exchange messages with each other. Finally, the computation and communication loads are reported in Table II.

C. Victoria Park Dataset

Finally, in this subsection, the performance of the proposed DMV-PHD-SLAM algorithm is assessed via the Victoria park dataset [51], a large-scale experimental scenario. The Victoria park dataset has been conceived for standard (single-vehicle) SLAM; thus, only one vehicle is deployed. For our experiments, we manually cut the dataset into four pieces, wherein each piece is assigned to a virtual vehicle in order to create an artificial four-vehicle scenario. Specifically, we allocated 13 000 control inputs to each vehicle. Note that the total number of control inputs in the dataset is 61 945, and that we did not cut the dataset sequentially, in order to ensure that the initial positions of the vehicles are spread all around the scenario. As a result, the vehicle trajectories are not strictly adjacent. Furthermore, in our simulations, the initial poses of vehicles are set by combining the result of running an SV-SLAM and the available intermittent GPS data (used to provide trajectory ground truth). Due to the fact that there is no landmark ground truth provided in this dataset, the focus is on comparison of localization performance.

In the Victoria park dataset, the vehicle was equipped with a LiDAR, the control inputs u_k were provided at a rate of 40 Hz, while the measurement outputs were supplied at a relatively slower rate of about 8 Hz. In the experiment, the FoV extension of all robots is set to $[0, \pi]\,\mathrm{rad} \times [0, 75]\,\mathrm{m}$, which means that the cells with range larger than 75 m in the raw data of LiDAR are omitted. The standard deviations of measurement noises are set to $\sigma_d = 0.3\,\mathrm{m}$ and $\sigma_\phi = 0.02\,\mathrm{rad}$, respectively. The standard deviations of model noises are set to $\sigma_\xi = 0.02\,\mathrm{m}$, $\sigma_\eta = 0.02\,\mathrm{m}$, and $\sigma_\theta = 0.001\,\mathrm{rad}$, respectively. Furthermore, it is supposed that the vehicles exchange their map data at the rate of 1 Hz, and vehicles can set up connections only when their relative distance is not larger than 350 m.

The performance of vehicle localization is qualitatively and quantitatively illustrated in Figs. 11 and 12, respectively. Note that since the GPS data are intermittent and contain outliers, the AMSE of vehicle localization in Fig. 12 is plotted only when available. It can be seen that, as map fusion is carried out, the accuracy of vehicle localization significantly improves. Furthermore, the results of collective mapping are illustrated in Fig. 13. It can be seen that, when running the proposed algorithm with $L = 1$, the estimated maps tend to reach consensus among vehicles, so that the landmarks located in the unexplored region of a vehicle can serve as anchors when the vehicle moves to that region, thus enhancing localization performance. Finally, the average complexity and SLAM performance of the considered methods is reported in Table III.

TABLE III
AVERAGE PERFORMANCE COMPARISON WITH THE VICTORIA PARK DATASET (PER RECURSION)

	DMV-PHD-SLAM	
	$L = 0$	$L = 1$
Local SLAM computing time $[s]$	1.76	2.79
Map fusion computing time $[s]$	–	0.27
Vehicle localization error $[m]$	2.44	1.85
Communication burden [Byte]	–	2748.3

Authorized licensed use limited to: Universita degli Studi di Firenze. Downloaded on January 27,2025 at 10:15:12 UTC from IEEE Xplore. Restrictions apply.

VIII. Conclusion

In this article, distributed multirobot (multivehicle) SLAM was addressed. Relying on the PHD-SLAM approach, GCI fusion was suitably modified in order to cope with robots with different and time-varying FoVs. Then, consensus was exploited in each teammate robot in order to spread information on the explored map. As a result, both mapping accuracy and the size of the explored zone were significantly enhanced with respect to a single robot. The performance of the proposed DMV-PHD-SLAM algorithm was verified on both simulated and experimental data. Potential future work will concern the following:

1) extended (nonpoint) landmarks, which possibly provide multiple measurements;
2) dynamic landmarks moving in the map;
3) DMV-SLAM based on more advanced multiobject filtering techniques, e.g., *cardinalized PHD*, *labeled multi-Bernoulli* filtering;
4) event-triggered data exchange strategies to save communication bandwidth;
5) case in which the relative robot poses are unknown, requiring sensor registration.

Appendix A
RFS Theory

From a probabilistic point of view, an RFS $\mathcal{M}$ is completely characterized by its *multiobject density* (MOD) $p(\mathcal{M})$. In this article, we consider specific RFSs having MOD of this form

$$p\left(\mathcal{M}\right) = |\mathcal{M}|!\, \rho\left(|\mathcal{M}|\right) \prod_{m \in \mathcal{M}} d(m) \tag{61}$$

where: $\rho(\cdot)$ is a *probability mass function* (PMF) defined over the set of nonnegative integers, $d(\cdot)$ is a PDF defined over the map space, and $|\cdot|$ denotes set cardinality. The PMF $\rho(n)$, $n \in \mathbb{N}$, characterizes the *cardinality distribution* and expresses the probability that the RFS $\mathcal{M}$ contains exactly n elements (i.e., the probability that the unknown map contains n landmarks). The PDF $d(m)$, $m \in \mathbb{M}$, is called *location density* and provides information on the distribution of the elements in the space $\mathbb{M}$. The location density $d(m)$ is usually multimodal, since it must account for the distribution of multiple elements inside the RFS. It is worth to point out that the factorial inside (61) accounts for the unordered character of the RFS, i.e., the fact that the ordering of the elements in the RFS is unessential. In addition, note that the product in (61) is taken to assume independence among the multiple objects.

Following [18], [19], and [21], the map is modeled as a multiobject Poisson process, whose cardinality PMF $\rho(\cdot)$ is a Poisson-distributed random variable with parameter λ. Accordingly, we have

$$\rho(n) = \frac{\lambda^n}{n!} e^{-\lambda} \tag{62}$$

and (61) is rewritten as

$$p\left(\mathcal{M}\right) = e^{-\lambda} \prod_{m \in \mathcal{M}} \lambda \cdot d(m). \tag{63}$$

All the information concerning a multiobject Poisson process like (63) can be summarized in the so-called PHD or intensity function

$$D(m) = \lambda \cdot d(m). \tag{64}$$

In fact, the MOD of a multiobject Poisson process can be exactly recovered from its PHD via the following relationship:

$$p\left(\mathcal{M}\right) = e^{-\int D(m)dm} \prod_{m \in \mathcal{M}} D(m)\,. \tag{65}$$

As pointed out in [53], the PHD $D(m)$ can be interpreted as local density of the number of elements at the map point m. Furthermore, given the PHD, the estimated number of elements inside a certain region $\overline{\mathbb{M}} \subseteq \mathbb{M}$ of the map space can be computed as

$$\widehat{N}\left(\overline{\mathbb{M}}\right) = \int_{\overline{\mathbb{M}}} D(m)dm \tag{66}$$

and the total number of map elements (landmarks) within the whole map space is given immediately by $\widehat{N} = \lambda$.

For the considered class of multiobject Poisson processes, the multiobject filtering problem can be accomplished by recursively computing the PHD at each time by means of the so-called *PHD filter* [44].

Appendix B
Proof of Theorem 1

Proof: The proof of the first result follows from the definition of MAP estimate. In fact, the MAP estimate of the unconditional PHD corresponding to the rth vehicle, at time t and after ℓ consensus steps, is obtained as

$$\widehat{D}^r_{t,\ell}(m) = D^{r,i^*}_{t,\ell}(m) \tag{67}$$

where

$$i^* = \arg \max_{i \in \{1,\ldots,M_r\}} w^{r,i}_t. \tag{68}$$

Since (30) holds for all $i \in \{1, 2, \ldots, M_r\}$, one can set $i = i^*$, where the value of i^* is given by (68), and thus obtain

$$D^{r,i^*}_{t,\ell}(m) = \left[\widetilde{D}^{r,i^*}_{t,\ell-1}(m)\right]^{\pi^{rr}_t} \prod_{s \in \mathcal{N}^r_t} \left[\widetilde{D}^s_{t,\ell-1}(m)\right]^{\pi^{rs}_t}. \tag{69}$$

Then, substituting into (67), we arrive at the conclusion of (31), which is indeed the ordinary consensus recursion for the PHD fusion.

In order to prove the second result, for the sake of clarity, let us define

$$D^r_i[\ell] \triangleq D^{r,i}_{t,\ell}(m) \tag{70}$$

$$D^r_*[\ell] \triangleq \prod_{s \in \mathcal{N}^r_t} \left[D^s_{t,\ell}(m)\right]^{\pi^{rs}_t} \tag{71}$$

$$\pi \triangleq \pi^{rr}_t \tag{72}$$

$$\bar{D} \triangleq \bar{D}_t(m) \tag{73}$$

Authorized licensed use limited to: Universita degli Studi di Firenze. Downloaded on January 27,2025 at 10:15:12 UTC from IEEE Xplore. Restrictions apply.

so that the consensus recursion can be expressed as

$$D_i^r[\ell] = D_i^r[\ell-1]^\pi \, D_*^r[\ell-1]. \tag{74}$$

Note that, if the ordinary consensus recursion converges (which is assumed), then

$$\lim_{\ell\to\infty} D_*^r[\ell] = \prod_{s\in\mathcal{N}^r} \bar{D}^{\pi_t^{rs}} = \bar{D}^{1-\pi}. \tag{75}$$

Now, taking the logarithm of both sides of (74) yields

$$\log D_i^r[\ell] = \pi \log D_i^r[\ell-1] + \log D_*^r[\ell-1]. \tag{76}$$

Then, setting $\xi_\ell = \log D_i^r[\ell]$ and $\upsilon_\ell = \log D_*^r[\ell]$ leads to the following dynamical system:

$$\xi_\ell = \pi\, \xi_{\ell-1} + \upsilon_{\ell-1} \tag{77}$$

which, since $\pi \in (0,1)$, is asymptotically stable and, moreover, is driven by an input signal, which is asymptotically constant

$$\lim_{\ell\to\infty} \upsilon_\ell = (1-\pi)\, \log \bar{D} \triangleq \bar{\upsilon}. \tag{78}$$

From standard LTI system theory, one can, therefore, conclude that ξ_ℓ admits the following limit:

$$\lim_{\ell\to\infty} \xi_\ell = \frac{\bar{\upsilon}}{1-\pi} = \log \bar{D}. \tag{79}$$

Finally, from the definition of ξ_ℓ, one obtains

$$\lim_{\ell\to\infty} D_i^r[\ell] = \bar{D}, \text{ for } i = 1,2,\ldots,M_r. \tag{80}$$

The proof can then be concluded by noting that such an analysis can be made for any $m \in \mathbb{M}$, so that pointwise convergence holds. ■

Appendix C
Distributed FastSLAM Algorithm Based on Consensus

Step 1 *Local filtering*

At time t, for each vehicle $r \in \mathcal{N}$, carry out the local SLAM algorithm of [73] to achieve the local posterior represented in particle form as

$$\mathcal{P}_t^r = \left\{\mathcal{P}_t^{r,i}\right\}_{i=1}^{M_r},$$

where

$$\mathcal{P}_t^{r,i} = \left\{\omega_t^{r,i}, \widehat{x}_t^{r,i}, \widehat{\mathcal{M}}_t^{r,i}\right\}.$$

$\widehat{\mathcal{M}}_t^{r,i} = \{(l_t^{r,i,k}, m_t^{r,i,k}, P_t^{r,i,k})\}_{k=1}^{N_t^{r,i}}$ denotes the detected landmarks of particle i at time t given the pose of vehicle as $\widehat{x}_t^{r,i}$, and $l_t^{r,i,k}$ denotes the label of kth landmark.

Step 2 *Consensus on maps*

Denote the index of the particle with largest weight at vehicle r as i_r^*; then, the map estimate of vehicle r at time t is obtained by the MAP criterion as $\widehat{\mathcal{M}}_t^r = \{(l_t^{r,k}, m_t^{r,k}, P_t^{r,k})\}_{k=1}^{N_t^{r,i_r^*}}$. Then, at vehicle $r \in \mathcal{N}$, after initializing consensus information as $\widehat{\mathcal{M}}_{t,0}^{r,i} = \widehat{\mathcal{M}}_t^{r,i}$ and $\widehat{\mathcal{M}}_{t,0}^r = \widehat{\mathcal{M}}_t^r$, a typical consensus iteration step ℓ is implemented as follows.

1) Broadcast $\widehat{\mathcal{M}}_{t,\ell-1}^r$ and then receive $\widehat{\mathcal{M}}_{t,\ell-1}^s$ from $s \in \mathcal{N}_t^r$.
2) For particle $i = 1,\ldots,M_r$, denote the label sets $\mathcal{L}_\ell^{r,i} = \{l_{t,\ell-1}^{r,i,k}\}_{k=1}^{N_{t,\ell}^{r,i}}$ and $\mathcal{L}_\ell^s = \{l_{t,\ell-1}^{s,k}\}_{k=1}^{N_{t,\ell}^s}$, for $s \in \mathcal{N}_t^r$. Let $\mathcal{L}_\ell^c = \mathcal{L}_\ell^{r,i} \bigcap \mathcal{L}_\ell^s$, and denote
$$\widetilde{\mathcal{M}}_{t,\ell}^{r,i} = \left\{\left(l_{t,\ell-1}^{r,i,k}, m_{t,\ell-1}^{r,i,k}, P_{t,\ell-1}^{r,i,k}\right)\right\}_{l_{t,\ell-1}^{r,i,k} \in \mathcal{L}_\ell^{r,i} \setminus \mathcal{L}_\ell^c}$$
$$\widetilde{\mathcal{M}}_{t,\ell}^{s} = \left\{\left(l_{t,\ell-1}^{s,k}, m_{t,\ell-1}^{s,k}, P_{t,\ell-1}^{s,k}\right)\right\}_{l_{t,\ell-1}^{s,k} \in \mathcal{L}_\ell^{s} \setminus \mathcal{L}_\ell^c}.$$
3) For $l_c \in \mathcal{L}_\ell^c$, fuse the state of its corresponding landmark according to (81) and (82), where $k : l_t^{r,i,k} = l_c$ and $k' : l_t^{s,k'} = l_c$. Denote
$$\widehat{\mathcal{M}}_{t,\ell}^{c} = \left\{\left(l_{t,\ell}^{r,i,k}, m_{t,\ell}^{r,i,k}, P_{t,\ell}^{r,i,k}\right)\right\}_{l_{t,\ell}^{r,i,k} \in \mathcal{L}_\ell^c}.$$
Then, the fused map of particle i of vehicle r is given as $\widehat{\mathcal{M}}_{t,\ell}^{r,i} = \widehat{\mathcal{M}}_{t,\ell}^{c} \bigcup \widetilde{\mathcal{M}}_{t,\ell}^{r,i} \bigcup \widetilde{\mathcal{M}}_{t,\ell}^{s}$.

$$P_{t,\ell}^{r,i,k} = \left[\pi_t^{rr}\left(P_{t,\ell-1}^{r,i,k}\right)^{-1} + \sum_{s\in\mathcal{N}_t^r} \pi_t^{rs}\left(P_{t,\ell-1}^{s,k'}\right)^{-1}\right]^{-1} \tag{81}$$

$$m_{t,\ell}^{r,i,k} = P_{t,\ell}^{r,i,k}\left[\pi_t^{rr}\left(P_{t,\ell-1}^{r,i,k}\right)^{-1} m_{t,\ell-1}^{r,i,k} + \sum_{s\in\mathcal{N}_t^r} \pi_t^{rs}\left(P_{t,\ell-1}^{s,k'}\right)^{-1} m_{t,\ell-1}^{s,k'}\right]. \tag{82}$$

References

[1] S. Thrun, W. Burgard, and D. Fox, *Probabilistic Robotics*. Cambridge, MA, USA: MIT Press, 2005.

[2] C. Stachniss, *Robotic Mapping and Exploration*. New York, NY, USA: Springer, 2009.

[3] S. Thrun *et al.*, "Stanley: The robot that won the DARPA grand challenge," *J. Field Robot.*, vol. 23, no. 9, pp. 661–692, 2006.

[4] C. F. Olson, L. H. Matthies, J. R. Wright, R. Li, and K. Di, "Visual terrain mapping for Mars exploration," *Comput. Vis. Image Understanding*, vol. 105, no. 1, pp. 73–85, 2007.

[5] S. Saeedi, M. Trentini, M. Seto, and H. Li, "Multiple-robot simultaneous localization and mapping—A review," *J. Field Robot.*, vol. 33, no. 1, pp. 3–46, 2015.

[6] S. Thrun, W. Burgard, and D. Fox, "A probabilistic approach to concurrent mapping and localization for mobile robots," *Mach. Learn.*, vol. 31, no. 3, pp. 29–53, 1998.

[7] H. Durrant-Whyte, and T. Bailey, "Simultaneous localization and mapping: Part I," *IEEE Robot. Autom. Mag.*, vol. 13, no. 2, pp. 99–110, Jun. 2006.

[8] G. Grisetti, R. Kummerle, C. Stachniss, and W. Burgard, "A tutorial on graph-based SLAM," *IEEE Intell. Transp. Syst. Mag.*, vol. 2, no. 4, pp. 31–43, Winter 2010.

[9] M. Montemerlo, S. Thrun, D. Koller, and B. Wegbreit, "FastSLAM: A factored solution to the simultaneous localization and mapping problem," in *Proc. Nat. Conf. Artif. Intell.*, 2002, pp. 593–598.

[10] M. Montemerlo, S. Thrun, D. Koller, and B. Wegbreit, "FastSLAM 2.0: An improved particle filtering algorithm for simultaneous localization and mapping that provably converges," in *Proc. Int. Joint Conf. Artif. Intell.*, 2003, pp. 1151–1156.

[11] C. Kim, R. Sakthivel, and W. K. Chung, "Unscented FastSLAM: A robust and efficient solution to the SLAM problem," *IEEE Trans. Robot.*, vol. 24, no. 4, pp. 808–820, Aug. 2008.

Authorized licensed use limited to: Universita degli Studi di Firenze. Downloaded on January 27,2025 at 10:15:12 UTC from IEEE Xplore. Restrictions apply.

[12] M. G. Dissanayake, P. Newman, S. Clark, H. F. Durrant-Whyte, and M. Csorba, "A solution to the simultaneous localization and map building (SLAM) problem," *IEEE Trans. Robot. Autom.*, vol. 17, no. 3, pp. 229–241, Jun. 2001.

[13] S. Huang and G. Dissanayake, "Convergence and consistency analysis for extended Kalman filter based SLAM," *IEEE Trans. Robot.*, vol. 23, no. 5, pp. 1036–1049, Oct. 2007.

[14] C. Cadena *et al.*, "Past, present, and future of simultaneous localization and mapping: Toward the robust-perception age," *IEEE Trans. Robot.*, vol. 32, no. 6, pp. 1309–1332, Dec. 2016.

[15] K. Y. Leung, F. Inostroza, and M. Adams, "Multifeature-based importance weighting for the PHD SLAM filter," *IEEE Trans. Aerosp. Electron. Syst.*, vol. 52, no. 6, pp. 2697–2714, Dec. 2016.

[16] R. P. Mahler, *Statistical Multisource-Multitarget Information Fusion*. Norwood, MA, USA: Artech House, 2007.

[17] R. P. Mahler, *Advances in Statistical Multisource-Multitarget Information Fusion*. Norwood, MA, USA: Artech House, 2014.

[18] J. Mullane, B.-N. Vo, M. D. Adams, and B.-T. Vo, "A random-finite-set approach to Bayesian SLAM," *IEEE Trans. Robot.*, vol. 27, no. 2, pp. 268–282, Apr. 2011.

[19] J. S. Mullane, B.-N. Vo, M. D. Adams, and B.-T. Vo, *Random Finite Sets for Robot Mapping & SLAM: New Concepts in Autonomous Robotic Map Representations* (Springer Tracts in Advanced Robotics), vol. 72. Berlin, Germany: Springer, 2011.

[20] C. S. Lee, D. E. Clark, and J. Salvi, "SLAM with dynamic targets via single-cluster PHD filtering," *IEEE J. Sel. Topics Signal Process.*, vol. 7, no. 3, pp. 543–552, Jun. 2013.

[21] M. Adams, B.-N. Vo, R. P. Mahler, and J. Mullane, "SLAM gets a PHD: New concepts in map estimation," *IEEE Robot. Autom. Mag.*, vol. 21, no. 2, pp. 26–37, Jun. 2014.

[22] H. Deusch, S. Reuter, and K. Dietmayer, "The labeled multi-Bernoulli SLAM filter," *IEEE Signal Process. Lett.*, vol. 22, no. 10, pp. 1561–1565, Oct. 2015.

[23] J. W. Fenwick, P. M. Newman, and J. J. Leonard, "Cooperative concurrent mapping and localization," in *Proc. IEEE Int. Conf. Robot. Autom.*, 2002, pp. 1810–1817.

[24] D. Moratuwage, B.-N. Vo, and D. Wang, "Collaborative multi-vehicle SLAM with moving object tracking," in *Proc. IEEE Int. Conf. Robot. Autom.*, 2013, pp. 5702–5708.

[25] D. Fox, J. Ko, K. Konolige, B. Limketkai, D. Schulz, and B. Stewart, "Distributed multirobot exploration and mapping," *Proc. IEEE*, vol. 94, no. 7, pp. 1325–1339, Jul. 2006.

[26] S. B. Williams, G. Dissanayake, and H. Durrant-Whyte, "Towards multi-vehicle simultaneous localisation and mapping," in *IEEE Int. Conf. Robot. Autom.*, 2002, pp. 2743–2748.

[27] A. Howard, "Multi-robot simultaneous localization and mapping using particle filters," *Int. J. Robot. Res.*, vol. 25, no. 12, pp. 1243–1256, 2006.

[28] X. S. Zhou and S. I. Roumeliotis, "Multi-robot SLAM with unknown initial correspondence: The robot rendezvous case," in *Proc. IEEE/RSJ Int. Conf. Intell. Robots Syst.*, 2006, pp. 1785–1792.

[29] A. Gil, Ó. Reinoso, M. Ballesta, and M. Juliá, "Multi-robot visual SLAM using a Rao-Blackwellized particle filter," *Robot. Auton. Syst.*, vol. 58, no. 1, pp. 68–80, 2010.

[30] D. Moratuwage, B.-N. Vo, and D. Wang, "A hierarchical approach to the multi-vehicle SLAM problem," in *Proc. Int. Conf. Inf. Fusion*, 2012, pp. 1119–1125.

[31] F. Zhang, H. Stahle, G. Chen, C. Buckl, and A. Knoll, "Multiple vehicle cooperative localization under random finite set framework," in *Proc. IEEE/RSJ Int. Conf. Intell. Robots Syst.*, 2013, pp. 1405–1411.

[32] D. Moratuwage, D. Wang, A. Rao, N. Senarathne, and H. Wang, "RFS collaborative multivehicle SLAM: SLAM in dynamic high-clutter environments," *IEEE Robot. Autom. Mag.*, vol. 21, no. 2, pp. 53–59, Jun. 2014.

[33] A. Cunningham, M. Paluri, and F. Dellaert, "DDF-SAM: Fully distributed SLAM using constrained factor graphs," in *Proc. IEEE/RSJ Int. Conf. Intell. Robots Syst.*, 2010, pp. 3025–3030.

[34] F. Dellaert, and M. Kaess, "Square root SAM: Simultaneous localization and mapping via square root information smoothing," *Int. J. Robot. Res.*, vol. 25, no. 12, pp. 1181–1203, 2006.

[35] A. Cunningham, V. Indelman, and F. Dellaert, "DDF-SAM 2.0: Consistent distributed smoothing and mapping," in *Proc. IEEE Int. Conf. Robot. Autom.*, 2013, pp. 5220–5227.

[36] K. Leung, T. Barfoot, and H. Liu, "Decentralized localization of sparsely-communicating robot networks: A centralized-equivalent approach," *IEEE Trans. Robot.*, vol. 26, no. 1, pp. 62–77, Feb. 2010.

[37] K. Leung, T. Barfoot, and H. Liu, "Decentralized cooperative SLAM for sparsely-communicating robot networks: A centralized-equivalent approach," *J. Intell. Robot. Syst.*, vol. 66, no. 3, pp. 321–342, 2012.

[38] C. Guo *et al.*, "Large-scale cooperative 3D visual-inertial mapping in a Manhattan world," in *Proc. IEEE Int. Conf. Robot. Autom.*, 2016, pp. 1071–1078.

[39] R. Aragues, J. Cortes, and C. Sagues, "Distributed consensus algorithms for merging feature-based maps with limited communication," *Robot. Auton. Syst.*, vol. 59, nos. 3/4, pp. 163–180, 2011.

[40] R. Aragues, J. Cortes, and C. Sagues, "Distributed consensus on robot networks for dynamically merging feature-based maps," *IEEE Trans. Robot.*, vol. 28, no. 4, pp. 840–854, Aug. 2012.

[41] L. Paull, M. Seto, J. Leonard, and H. Li, "Probabilistic cooperative mobile robot area coverage and its application to autonomous seabed mapping," *Int. J. Robot. Res.*, vol. 37, no. 1, pp. 21–45, 2018.

[42] S. G. Shahbandi and M. Magnusson, "2D map alignment with region decomposition," *Auton. Robots*, vol. 43, no. 5, pp. 1117–1136, 2019.

[43] M. Liggins II, C.-Y. Chong, D. Hall, and J. Llinas, *Distributed Data Fusion for Network-Centric Operations*. Boca Raton, FL, USA: CRC Press, 2012.

[44] R. P. Mahler, "Multitarget Bayes filtering via first-order multitarget moments," *IEEE Trans. Aerosp. Electron. Syst.*, vol. 39, no. 4, pp. 1152–1178, Oct. 2003.

[45] G. Battistelli and L. Chisci, "Kullback–Leibler average, consensus on probability densities, and distributed state estimation with guaranteed stability," *Automatica*, vol. 50, no. 3, pp. 707–718, 2014.

[46] G. Battistelli, L. Chisci, C. Fantacci, A. Farina, and A. Graziano, "Consensus CPHD filter for distributed multitarget tracking," *IEEE J. Sel. Topics Signal Process.*, vol. 7, no. 3, pp. 508–520, Jun. 2013.

[47] G. Battistelli, L. Chisci, and A. Laurenzi, "Random set approach to distributed multivehicle SLAM," *IFAC-PapersOnLine*, vol. 50, no. 1, pp. 2457–2464, 2017.

[48] J. Houssineau and D. Laneuville, "PHD filter with diffuse spatial prior on the birth process with applications to GM-PHD filter," in *Proc. Int. Conf. Inf. Fusion*, 2010, pp. 1–8.

[49] B. Ristic, D. Clark, B.-N. Vo, and B.-T. Vo, "Adaptive target birth intensity for PHD and CPHD filters," *IEEE Trans. Aerosp. Electron. Syst.*, vol. 48, no. 2, pp. 1656–1668, Apr. 2012.

[50] K. Y. Leung, Y. Halpern, T. D. Barfoot, and H. H. Liu, "The UITAS multi-robot cooperative localization and mapping dataset," *Int. J. Robot. Res.*, vol. 30, no. 8, pp. 969–974, 2011.

[51] J. Guivant and E. Nebot, "Simultaneous localization and map building: Test case for outdoor applications," [Online]. Available: http://www-personal.acfr.usyd.edu.au/nebot/publications/slam/IJRR_slam.htm

[52] L. Gao, G. Battistelli, and L. Chisci, "Random finite set based distributed multi-robot SLAM," *IEEE Dataport*, 2020. [Online]. Available: http://dx.doi.org/10.21227/fxya-bd26.

[53] O. Erdinc, P. Willett, and Y. Bar-Shalom, "The bin-occupancy filter and its connection to the PHD filters," *IEEE Trans. Signal Process.*, vol. 57, no. 11, pp. 4232–4246, Nov. 2009.

[54] B.-N. Vo, S. Singh, and A. Doucet, "Sequential Monte Carlo methods for multitarget filtering with random finite sets," *IEEE Trans. Aerosp. Electron. Syst.*, vol. 41, no. 4, pp. 1224–1245, Oct. 2005.

[55] R. P. Mahler, B. T. Vo, and B. N. Vo, "CPHD filtering with unknown clutter rate and detection profile," *IEEE Trans. Signal Process.*, vol. 59, no. 8, pp. 3497–3513, Aug. 2011.

[56] X. Wu, G. Huang, and J. Gao, "Adaptive noise variance identification for probability hypothesis density-based multi-target filter by variational Bayesian approximations," *IET Radar, Sonar Navigat.*, vol. 7, no. 8, pp. 895–903, 2013.

[57] B.-N. Vo and W.-K. Ma, "The Gaussian mixture probability hypothesis density filter," *IEEE Trans. Signal Process.*, vol. 54, no. 11, pp. 4091–4104, Nov. 2006.

[58] M. S. Arulampalam, S. Maskell, N. Gordon, and T. Clapp, "A tutorial on particle filters for online nonlinear/non-Gaussian Bayesian tracking," *IEEE Trans. Signal Process.*, vol. 50, no. 2, pp. 174–188, Feb. 2002.

[59] T. Li, M. Bolic, and P. M. Djuric, "Resampling methods for particle filtering: Classification, implementation, and strategies," *IEEE Signal Process. Mag.*, vol. 32, no. 3, pp. 70–86, May 2015.

[60] G. Battistelli, L. Chisci, C. Fantacci, A. Farina, and R. P. Mahler, "Distributed fusion of multitarget densities and consensus PHD/CPHD filters," *Proc. SPIE*, vol. 9474, 2015, Art. no. 94740E.

[61] C. Genest, and J. V. Zidek, "Combining probability distributions: A critique and an annotated bibliography," *Statist. Sci.*, vol. 1, no. 1, pp. 114–135, 1986.

Authorized licensed use limited to: Universita degli Studi di Firenze. Downloaded on January 27,2025 at 10:15:12 UTC from IEEE Xplore. Restrictions apply.

[62] R. P. Mahler, "Optimal/robust distributed data fusion: A unified approach," *Proc. SPIE*, vol. 4052, pp. 128–139, 2000.

[63] D. Clark, S. Julier, R. P. Mahler, and B. Ristić, "Robust multi-object sensor fusion with unknown correlations," in *Proc. Sens. Signal Process. Defence Conf.*, 2010, pp. 1–5.

[64] L. Xiao, S. Boyd, and S. Lall, "A scheme for robust distributed sensor fusion based on average consensus," in *Proc. 4th Int. Symp. Inf. Process. Sens. Netw.*, 2005, pp. 63–70.

[65] R. Olfati-Saber, J. A. Fax, and R. M. Murray, "Consensus and cooperation in networked multi-agent systems," *Proc. IEEE*, vol. 95, no. 1, pp. 215–233, Jan. 2007.

[66] M. Günay, U. Orguner, and M. Demirekler, "Chernoff fusion of Gaussian mixtures based on sigma-point approximation," *IEEE Trans. Aerosp. Electron. Syst.*, vol. 52, no. 6, pp. 2732–2746, Dec. 2016.

[67] L. Gao, G. Battistelli, L. Chisci, and P. Wei, "Distributed joint sensor registration and target tracking via sensor network," *Inf. Fusion*, vol. 46, pp. 218–230, 2019.

[68] L. Gao, G. Battistelli, L. Chisci, and P. Wei, "Distributed joint sensor registration and multitarget tracking via sensor network," *IEEE Trans. Aerosp. Electron. Syst.*, vol. 56, no. 2, pp. 1301–1317, Apr. 2020.

[69] L. Gao, G. Battistelli, L. Chisci, A. Gostar, and R. Hoseinnezhad, "Distributed joint mapping and registration with limited fields-of-view," in *Proc. Int. Conf. Control, Autom. Inf. Sci.*, 2019, pp. 1–6.

[70] D. Moratuwage, B.-N. Vo, D. Wang, and H. Wang, "Extending Bayesian RFS SLAM to multi-vehicle SLAM," in *Proc. Int. Conf. Control Autom. Robot. Vision*, 2012, pp. 638–643.

[71] R. P. Mahler, "The multisensor PHD filter, II: Erroneous solution via 'Poisson magic'," *Proc. SPIE*, vol. 7336, 2009, Art. no. 73360D.

[72] K. Panta, D. E. Clark, and B.-N. Vo, "Data association and track management for the Gaussian mixture probability hypothesis density filter," *IEEE Trans. Aerosp. Electron. Syst.*, vol. 45, no. 3, pp. 1003–1016, Jul. 2009.

[73] G. Grisetti, G. D. Tipaldi, C. Stachniss, W. Burgard, and D. Nardi, "Fast and accurate SLAM with Rao-Blackwellized particle filters," *Robot. Auton. Syst.*, vol. 55, no. 1, pp. 30–38, 2007.

[74] D. M. Rosen, C. DuHadway, and J. J. Leonard, "A convex relaxation for approximate global optimization in simultaneous localization and mapping," in *Proc. Int. Conf. Robot. Autom.*, 2015, pp. 5822–5829.

[75] R. Chatila and J. P. Laumond, "Position referencing and consistent world modeling for mobile robots," in *Proc. Int. Conf. Robot. Autom.*, 1985, pp. 138–145.

[76] H. W. Kuhn, "The Hungarian method for the assignment problem," *Naval Res. Logist. Quart.*, vol. 2, no. 1-2, pp. 83–97, 1955.

[77] D. Schuhmacher, B.-T. Vo, and B.-N. Vo, "A consistent metric for performance evaluation of multi-object filters," *IEEE Trans. Signal Process.*, vol. 56, no. 8, pp. 3447–3457, Aug. 2008.

[78] P. Barrios, M. Adams, K. Leung, F. Inostroza, G. Naqvi, and M. Orchard, "Metrics for evaluating feature-based mapping performance," *IEEE Trans. Robot.*, vol. 33, no. 1, pp. 198–213, Feb. 2017.

[79] M. Centenaro, L. Vangelista, A. Zanella, and M. Zorzi, "Long-range communications in unlicensed bands: The rising stars in the IoT and smart city scenarios," *IEEE Wireless Commun.*, vol. 23, no. 5, pp. 60–67, Oct. 2016.

Lin Gao received the M.S. and Ph.D. degrees in electrical engineering from the University of Electronic Science and Technology of China, Chengdu, China, in 2014 and 2018, respectively.

He is currently a Research Fellow with the Department of Information Engineering, University of Florence, Florence, Italy. His research interests include statistical signal processing, multisensor multitarget tracking, information fusion, and multivehicle simultaneous localization and mapping.

Giorgio Battistelli received the Laurea degree in electronic engineering and the Ph.D. degree in robotics from the University of Genoa, Genoa, Italy, in 2000 and 2004, respectively.

From 2004 to 2006, he was a Research Associate with the Dipartimento di Informatica, Sistemistica e Telematica, University of Genoa. Since 2006, he has been with the University of Florence, Florence, Italy, where he is currently a Full Professor of Automatic Control with the Department of Information Engineering. His current research interests include adaptive and learning systems, real-time control reconfiguration, linear and nonlinear estimation, hybrid systems, sensor networks, and data fusion.

Dr. Battistelli was a member of the Editorial Boards of the *IFAC Journal Engineering Applications of Artificial Intelligence* and the IEEE TRANSACTIONS ON NEURAL NETWORKS AND LEARNING SYSTEMS. He is an Associate Editor for the IEEE CONTROL SYSTEMS LETTERS, *Sensors*, and *Nonlinear Analysis: Hybrid Systems*.

Luigi Chisci (Senior Member, IEEE) was born in Florence, Italy, in 1959. He received the M.S. degree in electrical engineering from the University of Florence, Florence, Italy, in 1984, and the Ph.D. degree in systems engineering from the University of Bologna, Bologna, Italy, in 1989.

Since December 2004, he has been a Full Professor of Control Engineering with the University of Florence. His educational and research career have been in the area of control and systems engineering. His research interests have spanned over adaptive control and signal processing, algorithms and architectures for real-time control and signal processing, recursive identification, filtering and estimation, and predictive control. His current research interests include networked estimation, multitarget multisensor tracking, multiagent systems, and sensor data fusion.

Dr. Chisci was on the Conference Editorial Board of the IEEE Control Systems Society as an Associate Editor from 2000 to 2008. He is an Associate Editor for the *International Journal of Adaptive Control and Signal Processing*.

Authorized licensed use limited to: Universita degli Studi di Firenze. Downloaded on January 27,2025 at 10:15:12 UTC from IEEE Xplore. Restrictions apply.